IEEE Access
Multidisciplinary | Rapid Review | Open Access Journal

Received May 13, 2021, accepted June 14, 2021, date of publication June 24, 2021, date of current version July 9, 2021.

Digital Object Identifier 10.1109/ACCESS.2021.3092021

Robust Generalized Labeled Multi-Bernoulli Filter for Multitarget Tracking With Unknown Non-Stationary Heavy-Tailed Measurement Noise

LIMING HOU[1], FENG LIAN[1], SHUNCHENG TAN[2,3], CONGAN XU[3], AND GIUSEPPE THADEU FREITAS DE ABREU[4], (Senior Member, IEEE)

[1]Ministry of Education Key Laboratory for Intelligent Networks and Network Security, School of Electronics and Information Engineering, Xi'an Jiaotong University, Xi'an 710049, China
[2]Nanjing Research Institute of Electronics Technology, Nanjing 210039, China
[3]Institute of Information Fusion, Naval Aviation University, Yantai 264001, China
[4]Department of Computer Science and Electronic Engineering, Jacobs University Bremen, 28759 Bremen, Germany

Corresponding author: Feng Lian (lianfeng1981@xjtu.edu.cn)

This work was supported in part by the National Natural Science Foundation of China under Grant 61671462 and Grant 61473217, in part by the China Scholarship Council Foundation under Grant 201906280272, and in part by the Natural Science Basic Research Program of Shaanxi under Grant 2020JQ-073.

ABSTRACT A robust generalized labeled multi-Bernoulli (GLMB) filter is presented to perform multitarget tracking (MTT) with unknown non-stationary heavy-tailed measurement noise (HTMN). The HTMN is modeled as a multivariate Student's t-distribution with unknown and time-varying mean. The proposed filter relaxes the restrictive assumption that the mean of HTMN is zero, and can effectively deal with MTT under the condition that the mean of HTMN is unknown and time-varying. The variational Bayesian (VB) approximation is applied in the GLMB filtering framework with the augmented state. The marginal likelihood function is obtained via minimizing the Kullback-Leibler divergence by the variational lower bound. The simulation results demonstrate that the proposed filter can effectively track multiple targets in both linear and nonlinear scenarios when the mean of HTMN is unknown and time-varying.

INDEX TERMS Generalized labeled multi-Bernoulli filter, multitarget tracking (MTT), variational Bayesian (VB), non-stationary, heavy-tailed measurement noise (HTMN), unknown and time-varying mean.

I. INTRODUCTION

Multitarget tracking (MTT) involves the estimation of the number of unknown and time-varying targets, their trajectories, and kinematic states in real-time from the measurement sequences in the presence of uncertainties in detection, clutter, and data associations. So far, three of the most prominent MTT approaches have been used to perform MTT, such as Joint Probabilistic Data Association (JPDA) [1], [2], Multiple Hypotheses Tracking (MHT) [3], and Random Finite Set (RFS) [4], [5].

The RFS approach is essentially a multitarget Bayesian (MTB) filter that recursively propagates the posterior multitarget densities. To alleviate the computational complexity from the joint probability distribution and multiple integrals, three approximate filters, including the probability hypothesis density (PHD) filter [6], cardinality PHD (CPHD) filter [7], and multitarget multi-Bernoulli (MeMBer) [4], [8] filter, have been developed. However, the aforementioned filters are not true multitarget trackers, since they cannot obtain distinguishable target trajectories. To overcome this problem, a rigorous generalized labeled multi-Bernoulli (GLMB) filter is presented in [9], [10]. By utilizing a first-order approximate matching model to approximate the GLMB posterior distribution to the labeled multi-Bernoulli (LMB) distribution, the LMB filter is proposed in [11]. An efficient approximation of the GLMB filter which preserves both the PHD and cardinality distribution of the labeled posterior is developed in [12]. Note that an efficient implementation is proposed in [13], which combines the prediction and updating into a single step and further implements only one truncation for each iteration. Subsequently, a much cheaper truncation based on Gibbs sampling is presented in [14]. This filter also combines the GLMB filter prediction and update steps

The associate editor coordinating the review of this manuscript and approving it for publication was Halil Ersin Soken.

TABLE 1. Acronyms and nomenclatures.

Notations	Definitions
HTMN	Heavy-tailed measurement noise
PDF	Probability density function
DOF	Degree of freedom
J-GLMB	GLMB filter with joint prediction and update
NGIWG	Gaussian Gamma inverse-Wishart Gamma
NNIWGG	Gaussian Gaussian-inverse-Wishart Gamma Gamma
GM	Gaussian mixture
STM	Student's t mixture
$\mathrm{E}[\cdot]$	Mathematical expectation operation
$\mathrm{St}(\cdot;\mu,R,v)$	Multivariate Student's-t PDF with mean vector μ, scale matrix R and DOF v
$\mathrm{N}(\cdot;m,P)$	Multivariate Gaussian PDF with mean vector m and covariance matrix P
$\mathrm{G}(\cdot;a,b)$	Gamma PDF with shape parameter a and scale parameter b
$\mathrm{IW}(\cdot;\omega,P)$	Inverse-Wishart PDF with DOF ω and inverse scale matrix P
$\mathrm{tr}(\cdot)$	Trace operation
$\ln(\cdot)$	Natural logarithmic operation
$\mathrm{KL}(q \parallel p)$	Kullback-Leibler divergence between q and p
$\Gamma(\cdot)$	Gamma function

into a single joint operation and will be referred to as the 'J-GLMB filter' in the rest of the paper. Its complexity is linear in the number of measurements and quadratic in the number of hypothesized labels, whereas the original solution in [13] is cubic at best in both cases. The J-GLMB filter has been applied not only to extended target tracking [15] and multi-sensor MTT [16], [17], but also to large-scale multi-object tracking [18] and multiple objects tracking in unknown backgrounds, such as clutter rate and detection probability [19]. Furthermore, a multi-scan version of the J-GLMB filter is proposed to perform multi-object smoothing in [20].

For the MTT applications, it is generally assumed that the measurement noise is a zero-mean Gaussian white noise sequence. However, in radar tracking systems, the measurement tends to be disturbed by heavy-tailed measurement noise (HTMN), which is a non-Gaussian noise with a heavy-tailed probability density function (PDF) caused by the irregular changes of electromagnetic wave reflections [21]. The HTMN may lead to a significant decline in the tracking performance of those filters using the traditional Gaussian modeling scheme [22], [23]. At present, the modeling method of HTMN is mainly realized through the combination of Gaussian noise and other noise distributions. The HTMN was described as a weighted sum of two Gaussian distributions in [22]–[26]. One Laplace distribution and one small variance Gaussian distribution were employed to characterize the HTMN together in [21], [27] and [28]. Moreover, a Student's t-distribution mixture GLMB filter, in which both the process and measurement noises are modeled as the Student's t-distributions with zero-mean, known scalar matrix and degrees of freedom, is proposed in [29] to deal with heavy-tailed process noise and measurement noise in nonlinear MTT systems. A PHD filter based on the Student's t-distribution for MTT with HTMN is proposed in [30]. The variational Bayesian (VB) approach is utilized to deal with significant intractability caused by the Student's t-distribution in the PHD filtering framework. Similarly, a novel CPHD filter for extended targets tracking with HTMN is presented in [31]. To obtain multitarget trajectories, a Gaussian (Normal) Gamma inverse Wishart Gamma distribution mixtures LMB (NGIWG-LMB) filter is proposed in [32] to perform MTT for stationary HTMN, as well as a Student's t mixture LMB (STM-LMB) filter for MTT with heavy-tailed process and measurement noises is presented in [33]. Furthermore, a novel LMB filter is presented in [34] for jump Markov systems to track multiple maneuvering targets under HTMN.

However, in practice, the measurement bias resulted from sensor faults may lead to non-stationary measurement noise. For the HTMN with unknown and time-varying measurement bias, Huang *et al.* modeled the measurement noise as a Student's t-inverse-Wishart distribution and proposed a robust Kalman filter which can adaptively estimate the measurement bias in [35]. However, the degree of freedom (DOF) of the noise distribution is a known fixed value. Actually, the DOFs of noises are usually unknown. Also, the Gaussian-Gamma distribution is selected as the conjugate prior distribution for a univariate Gaussian distribution in which the mean and precision are both unknown, but it is not suitable for a multivariate Gaussian distribution with unknown mean and precision. To the best of the authors' knowledge, there is no research on MTT problems under unknown non-stationary HTMN.

In this paper, a robust J-GLMB filter based on the Student's t-distribution and VB approach is presented for MTT with unknown non-stationary HTMN. The measurement noise is modeled as a multivariate Student's t-distribution with unknown and time-varying mean. The Student's t-distribution is written as the mixtures of Gaussian, Gaussian-inverse-Wishart, and Gamma distributions, of which the auxiliary variable is modeled as Gamma distribution conditional on the DOF. Besides, the DOF is also modeled by the Gamma distribution. To address the problem of MTT with unknown non-stationary HTMN, the target state is augmented by the parameters of the Student's t-distribution with unknown and time-varying mean, kinematic state, and target label. And then the predicted and updated intensities are represented as Gaussian, Gaussian-inverse-Wishart, Gamma, and Gamma (NNIWGG) distribution mixtures. In the update step, the VB approach is employed to decouple the augmented state. To obtain a closed-form implementation of the proposed robust J-GLMB filter, the updated density is derived via the VB approach to ensure that it has the same form as the prediction one. Furthermore, the VB lower bound is utilized to approximate the predictive likelihood. Simulation results show that the effectiveness of the proposed robust J-GLMB filter under unknown non-stationary HTMN and its robustness compared with the existing filters.

The paper is organized as follows. Section II develops a Bayesian hierarchical model for the Student's t-distribution with unknown and time-varying mean and provides a brief introduction to the GLMB RFS and GLMB filter. Section III presents the proposed robust J-GLMB filter based on the Student's t-distribution for unknown non-stationary HTMN. Simulation results and comparisons are followed in Section IV. Finally, conclusions are drawn in Section V.

II. BACKGROUND

A. PROBLEM FORMULATION

A linear state-space model at time k can be formulated using the following equations:

$$\boldsymbol{x}_k = \boldsymbol{F}\boldsymbol{x}_{k-1} + \boldsymbol{w}_{k-1} \tag{1}$$

$$\boldsymbol{z}_k = \boldsymbol{H}\boldsymbol{x}_k + \boldsymbol{\varepsilon}_k \tag{2}$$

where $\boldsymbol{x}_k \in \mathbb{R}^n$ and $\boldsymbol{z}_k \in \mathbb{R}^m$ are the state and measurement vectors, respectively; and $\boldsymbol{F} \in \mathbb{R}^{n\times n}$ and $\boldsymbol{H} \in \mathbb{R}^{m\times n}$ represent the state transition and observation matrices, respectively, and $\boldsymbol{w}_k \in \mathbb{R}^n$ denotes the Gaussian process noise with a mean of $\mathrm{E}\{\boldsymbol{w}_k\} = \boldsymbol{0}$ and a covariance matrix of $\mathrm{E}\{\boldsymbol{w}_k\boldsymbol{w}_l^{\mathrm{T}}\} = \boldsymbol{Q}_k\delta_{kl}$, where δ_{kl} is the Kronecker Delta function; and $\boldsymbol{\varepsilon}_k \in \mathbb{R}^m$ denotes the non-stationary HTMN. The initial state $\boldsymbol{x}_0 \in \mathbb{R}^n$ has a Gaussian distribution with mean $\boldsymbol{m}_0$ and covariance matrix $\boldsymbol{P}_0$. It is assumed that $\boldsymbol{x}_0$, $\boldsymbol{w}_k$, and $\boldsymbol{\varepsilon}_k$ are mutually independent.

The research shows that the Student's t-distribution can better model the HTMN [36]. Compared with the Gaussian distribution, the Student's t-distribution is more suitable to match the heavy-tailed non-Gaussian distribution. Therefore, the existing filters generally employ the Student's t-distribution with zero mean to model the HTMN [30]–[34]. However, the sensor failure or severe disturbance often leads to an unknown measurement bias, which makes the heavy-tailed noise non-stationary [35]. To this end, we adopt the Student's t-distribution with unknown and time-varying mean to describe the non-stationary HTMN. Therefore, the multivariate Student's t-distribution [37] is utilized to describe $\boldsymbol{\varepsilon}_k$, that is,

$$p(\boldsymbol{\varepsilon}_k) = \mathrm{St}(\boldsymbol{\varepsilon}_k; \boldsymbol{\mu}, \boldsymbol{R}, v) \tag{3}$$

with

$$\mathrm{St}(\boldsymbol{\varepsilon}_k; \boldsymbol{\mu}, \boldsymbol{R}, v) = \frac{\Gamma\left(\frac{v+m}{2}\right)\left[1 + \frac{1}{v}(\boldsymbol{\varepsilon}_k - \boldsymbol{\mu})^{\mathrm{T}}\boldsymbol{R}^{-1}(\boldsymbol{\varepsilon}_k - \boldsymbol{\mu})\right]^{-\frac{v+m}{2}}}{(\pi v)^{\frac{m}{2}}\Gamma(\frac{v}{2})\sqrt{\det(\boldsymbol{R})}} \tag{4}$$

where $\boldsymbol{\mu}$, $\boldsymbol{R}$, and v represent the mean vector, the scale matrix and the DOF, respectively, and $\Gamma(\cdot)$ denotes the Gamma function and $\det(\cdot)$ denotes the determinant operator. When $v \to \infty$, the Student's t-distribution reduces to a Gaussian distribution with mean vector $\boldsymbol{\mu}$ and covariance matrix $\boldsymbol{R}$. That is the Student's t-distribution can be regarded as a generalized Gaussian distribution. It should be noted that $\boldsymbol{\mu}$ is unknown and time-varying, and $\boldsymbol{R}$ and v are unknown in this paper.

B. BAYESIAN HIERARCHICAL MODEL

To derive the closed form expressions of the posterior PDF for (1) and (2), it is necessary to model the likelihood $p(\boldsymbol{z}_k|\boldsymbol{x}, \boldsymbol{\mu}, \boldsymbol{R}, v)$ and the one-step predicted PDF $p(\boldsymbol{x}|\boldsymbol{z}_{1:k-1})$. According to (2) and (3), $p(\boldsymbol{z}_k|\boldsymbol{x}, \boldsymbol{\mu}, \boldsymbol{R}, v)$ is formulated as

$$p(\boldsymbol{z}_k|\boldsymbol{x}, \boldsymbol{\mu}, \boldsymbol{R}, v) = \mathrm{St}(\boldsymbol{z}_k; \boldsymbol{H}\boldsymbol{x} + \boldsymbol{\mu}, \boldsymbol{R}, v). \tag{5}$$

However, due to the non-stationarity of HTMN, the mean vector $\boldsymbol{\mu}$, scale matrix $\boldsymbol{R}$ and DOF v cannot be obtained accurately. To this end, the VB approach is utilized to estimate the above unknown parameters adaptively. The Gaussian-inverse-Wishart distribution [38] is selected as the prior distribution for $\boldsymbol{\mu}$ and $\boldsymbol{R}$ to ensure that the posterior PDF and the prior PDF have the same form, that is,

$$p(\boldsymbol{\mu}, \boldsymbol{R}|\boldsymbol{z}_{1:k-1}) = \mathrm{N}(\boldsymbol{\mu}; \boldsymbol{\eta}_{k|k-1}, \beta_{k|k-1}\boldsymbol{R}) \times \mathrm{IW}(\boldsymbol{R}; t_{k|k-1}, \boldsymbol{T}_{k|k-1}) \tag{6}$$

where $\boldsymbol{\eta}_{k|k-1}$, $\beta_{k|k-1}\boldsymbol{R}$, $t_{k|k-1}$ and $\boldsymbol{T}_{k|k-1}$ are, respectively, the mean vector, covariance matrix, DOF and the inverse scale matrix of $p(\boldsymbol{\mu}, \boldsymbol{R}|\boldsymbol{z}_{1:k-1})$.

Similarly, the Gamma distribution is selected as the prior distribution of v,

$$p(v|\boldsymbol{z}_{1:k-1}) = \mathrm{G}(v; a_{k|k-1}, b_{k|k-1}) \tag{7}$$

where $a_{k|k-1}$ and $b_{k|k-1}$ denote the shape parameter and rate parameter of $p(v|\boldsymbol{z}_{1:k-1})$, respectively.

Under the Gaussian approximation to posterior PDF, the one-step predicted PDF is updated as a Gaussian distribution using the Chapman-Kolmogorov equation, i.e.,

$$p(\boldsymbol{x}|\boldsymbol{z}_{1:k-1}) = \mathrm{N}(\boldsymbol{x}; \boldsymbol{m}_{k|k-1}, \boldsymbol{P}_{k|k-1}) \tag{8}$$

where the state mean vector $\boldsymbol{m}_{k|k-1}$ and the covariance matrix $\boldsymbol{P}_{k|k-1}$ are obtained by the time-update step of Kalman filter as follows,

$$\boldsymbol{m}_{k|k-1} = \boldsymbol{F}\boldsymbol{m}_{k-1} \tag{9}$$

$$\boldsymbol{P}_{k|k-1} = \boldsymbol{F}\boldsymbol{P}_{k-1}\boldsymbol{F}^{\mathrm{T}} + \boldsymbol{Q}_k. \tag{10}$$

Assume that $\boldsymbol{x}$, $\boldsymbol{\mu}$, $\boldsymbol{R}$ and v are mutually independent. And in order to derive $p(\boldsymbol{\mu}, \boldsymbol{R}|\boldsymbol{z}_{1:k-1})$ and $p(v|\boldsymbol{z}_{1:k-1})$, a forgetting factor $\rho \in (0, 1]$ is used to describe the dynamic uncertainty of $\boldsymbol{\mu}$, $\boldsymbol{R}$ and v. Under the principle of keeping the expected value unchanged and the variance increased by ρ^{-1} times, and according to the properties of Gaussian distribution, inverse-Wishart distribution and Gamma distribution, the dynamic models of each parameter can be obtained

$$\boldsymbol{\eta}_{k|k-1} = \boldsymbol{\eta}_{k-1}, \quad \beta_{k|k-1} = \beta_{k-1}/\rho \tag{11}$$

$$t_{k|k-1} = \rho t_{k-1}, \quad \boldsymbol{T}_{k|k-1} = \rho\boldsymbol{T}_{k-1} \tag{12}$$

$$a_{k|k-1} = \rho a_{k-1}, \quad b_{k|k-1} = \rho b_{k-1}. \tag{13}$$

A new state-space model based on the multivariate Student's t-distribution with unknown and time-varying mean

incorporates (5)-(8). However, considering the Student's t-distribution does not have a rigorous closed-form solution, the posterior PDF is not available. To solve the problem, by introducing an auxiliary variable λ, the likelihood $p(\boldsymbol{z}_k|\boldsymbol{x}, \boldsymbol{\mu}, \boldsymbol{R}, \lambda)$ as shown in (5) can be expressed as the following Bayesian hierarchical model [39],

$$p(\boldsymbol{z}_k|\boldsymbol{x}, \boldsymbol{\mu}, \boldsymbol{R}, \lambda) = \mathrm{N}(\boldsymbol{z}_k; \boldsymbol{H}\boldsymbol{x} + \boldsymbol{\mu}, \boldsymbol{R}/\lambda) \tag{14}$$

$$p(\lambda|v) = \mathrm{G}(\lambda; v/2, v/2). \tag{15}$$

To sum up, the state estimation problem with unknown non-stationary HTMN is transformed into the state estimation in a hierarchical model based on the multivariate Student's t-distribution with (6)-(8), and (14)-(15). And it can be seen from (15) that λ can be completely determined by v.

Remark: Bayesian hierarchical model is a structured statistical model which utilizes the Bayesian method to estimate posterior distribution parameters. It can be used to establish a hierarchical model for complex statistical problems to avoid overfitting problems caused by excessive parameters.

C. LABELED RFS AND GLMB FILTER

In order to incorporate target trajectories in the framework of the MTB filtering, the labeled RFS is introduced in [9]. For each target, the state $x \in \mathbb{X}$ is augmented by a unique label $\ell = (k, i)$, where k is the time of birth and $i \in \mathbb{N}$ is a unique index to distinguish targets born at time k. Then, the label space of a new target born at k time is denoted as $\mathbb{L}_k = \{k\} \times \mathbb{N}$. Consequently, the labeled state $\boldsymbol{x} = (x, \ell) \in \mathbb{X} \times \mathbb{L}_k$ can denote a new target born at time k, where $\mathbb{X}$ and $\mathbb{L}$ represent the state space and label space, respectively. Likewise, the labeled multitarget state is denoted as $\boldsymbol{X} = \{\boldsymbol{x}_1, \ldots, \boldsymbol{x}_n\} = \{(x_1, \ell_1), \ldots, (x_n, \ell_n)\} \subseteq \mathbb{X} \times \mathbb{L}$, where $\ell_1, \ldots, \ell_n$ are distinct from each other.

Define the projection $\mathcal{L} : \mathbb{X} \times \mathbb{L} \to \mathbb{L}$. For a labeled state $\boldsymbol{x}$, $\mathcal{L}(\boldsymbol{x}) = \mathcal{L}((x, \ell)) = \ell$. Likewise, for a labeled multitarget state $\boldsymbol{X}$, $\mathcal{L}(\boldsymbol{X}) = \{\mathcal{L}(\boldsymbol{x}) : \boldsymbol{x} \in \boldsymbol{X}\}$, and the labels must be distinct, i.e., $\delta_{|\boldsymbol{X}|}(|\mathcal{L}(\boldsymbol{X})|) = 1$. For simplicity, the distinct label indicator is defined as $\Delta(\boldsymbol{X}) = \delta_{|\boldsymbol{X}|}(|\mathcal{L}(\boldsymbol{X})|)$.

According to [9], [10], a GLMB RFS is distributed as

$$\pi(\boldsymbol{X}) = \Delta(\boldsymbol{X}) \sum_{I,\xi} \omega^{(I,\xi)} \delta_I[\mathcal{L}(\boldsymbol{X})] \left[p^{(\xi)}\right]^{\boldsymbol{X}} \tag{16}$$

where $I \in \mathcal{F}(\mathbb{L})$ is a set of track labels, $\xi \in \Xi$ denotes a history of association maps, each $p^{(\xi)}(\cdot, \ell)$ is a probability density on $\mathbb{X}$, and each $\omega^{(I,\xi)}$ is non-negative with $\sum_{I,\xi} \omega^{(I,\xi)} = 1$.

Each component (I, ξ) in (16) consists of a weight $\omega^{(I,\xi)}$ that only depends on the labels of the multitarget state $\boldsymbol{X}$ and a multitarget exponential $\left[p^{(\xi)}\right]^{\boldsymbol{X}}$, which is the product of the single target probability densities.

In the original GLMB filter, if the prior multitarget density is a GLMB of the form (16), then the predicted and posterior multitarget densities are still GLMBs of the forms

$$\pi_+(\boldsymbol{X}_+) = \Delta(\boldsymbol{X}_+) \sum_{I_+,\xi} \omega_+^{(I_+,\xi)} \delta_{I_+}[\mathcal{L}(\boldsymbol{X}_+)] [p_+^{(\xi)}]^{\boldsymbol{X}_+} \tag{17}$$

$$\pi_{\boldsymbol{Z}_+}(\boldsymbol{X}) \propto \Delta(\boldsymbol{X}) \sum_{I,\xi} \sum_{\theta} \omega_{\boldsymbol{Z}_+}^{(I,\xi,\theta)} \delta_I[\mathcal{L}(\boldsymbol{X})] \left[p_{\boldsymbol{Z}_+}^{(\xi,\theta)}\right]^{\boldsymbol{X}} \tag{18}$$

where θ is the association map, $\Theta(I)$ denotes the set of association maps with label domain I. For more details, the readers can refer to [9], [10].

III. ROBUST J-GLMB FILTER FOR UNKNOWN NON-STATIONARY HTMN

To estimate the kinematic state of the target and parameters of the Student's t-distribution, they are expressed as an augmented target state in a hybrid state space, and the corresponding joint PDF can be expressed as an NNIWGG model. However, in the Bayesian filtering framework, there is no analytical solution for the joint posterior PDF, so the VB approach is used to approximate it. Furthermore, the single target spatial PDF is denoted as the NNIWGG model and propagated under the framework of the J-GLMB filter. By minimizing the Kullback-Leibler divergence, the variational lower bound is taken as the approximate solution of the marginal likelihood. Therefore, we introduce this NNIWGG density to give an implementation of the extended version of the J-GLMB filter, referred to as the NNIWGG-J-GLMB filter in this paper.

A. SINGLE TARGET TRACKING WITH THE NNIWGG MODEL

In this paper, the target state augmentation approach is adopted in the J-GLMB filter. Therefore, the augmented state is defined as follows

$$\boldsymbol{\zeta} \triangleq (\boldsymbol{x}, \boldsymbol{\mu}, \boldsymbol{R}, \lambda, v) \in \mathbb{R}^* \tag{19}$$

where $\boldsymbol{\zeta}$ denotes an augmented state, $\mathbb{R}^*$ is the hybrid state space and $\mathbb{R}^* = \mathbb{R}^n \times \mathbb{R}^m \times \mathbb{R}_+^m \times \mathbb{R}^+ \times \mathbb{R}^+$, $\mathbb{R}^n$ and $\mathbb{R}^m$ represent n-dimensional and m-dimensional real vector space respectively, $\mathbb{R}_+^m$ is the space of $m \times m$ positive-definite matrices, $\mathbb{R}^+$ denotes the space of positive real numbers, $\times$ represents the Cartesian product.

According to the Bayes's rule, given the measurement set $\boldsymbol{z}_k$ at time k, the joint posterior PDF $p(\boldsymbol{\zeta}|\boldsymbol{z}_{1:k})$ can be calculated by

$$p(\boldsymbol{\zeta}|\boldsymbol{z}_{1:k}) = \frac{p(\boldsymbol{z}_k|\boldsymbol{\zeta}) p(\boldsymbol{\zeta}|\boldsymbol{z}_{1:k-1})}{p(\boldsymbol{z}_k|\boldsymbol{z}_{1:k-1})} \tag{20}$$

where $p(\boldsymbol{z}_k|\boldsymbol{z}_{1:k-1}) = \int p(\boldsymbol{z}_k|\boldsymbol{\zeta}) p(\boldsymbol{\zeta}|\boldsymbol{z}_{1:k-1}) d\boldsymbol{\zeta}$ is the marginal likelihood.

It can be seen from Section II. B that the posterior PDF of a single target with the augmented state can be expressed as the NNIWGG model in the hybrid state space, i.e.,

$$\begin{aligned} p(\boldsymbol{\zeta}) &= p(\boldsymbol{x}) p(\boldsymbol{\mu}|\boldsymbol{R}) p(\boldsymbol{R}) p(\lambda|v) p(v) \\ &= \mathrm{N}(\boldsymbol{x}; \boldsymbol{m}, \boldsymbol{P}) \mathrm{N}(\boldsymbol{\mu}; \boldsymbol{\eta}, \beta\boldsymbol{R}) \mathrm{IW}(\boldsymbol{R}; t, \boldsymbol{T}) \\ &\quad \times \mathrm{G}(\lambda; v/2, v/2) \mathrm{G}(v; a, b) \\ &\triangleq \mathrm{NNIWGG}(\boldsymbol{\zeta}; \boldsymbol{\phi}) \end{aligned} \tag{21}$$

where $\boldsymbol{\phi} = (\boldsymbol{m}, \boldsymbol{P}, \boldsymbol{\eta}, \beta, t, \boldsymbol{T}, a, b)$ is a variational parameter set of the NNIWGG density.

To formulate the recursive estimate of both target state and Student's t-distribution parameters, we assume that the single target transition density is Markovian and can be factorized as

$$f(\boldsymbol{\zeta}|\boldsymbol{\zeta}') = f(\boldsymbol{x}|\boldsymbol{x}')f(\boldsymbol{\mu}|\boldsymbol{\mu}')f(\boldsymbol{R}|\boldsymbol{R}')f(\lambda|v)f(v|v') \tag{22}$$

where $f(\boldsymbol{\zeta}|\boldsymbol{\zeta}')$ denotes the transition density of the augmented state. Then, the Bayesian prediction for an NNIWGG form can be given by Lemma 1.

Lemma 1: Given the joint prior PDF $p(\boldsymbol{\zeta}') = \text{NNIWGG}(\boldsymbol{\zeta}'; \phi_{k-1})$ at time $k-1$, where $\phi_{k-1} = (\boldsymbol{m}_{k-1}, \boldsymbol{P}_{k-1}, \boldsymbol{\eta}_{k-1}, \beta_{k-1}, t_{k-1}, \boldsymbol{T}_{k-1}, a_{k-1}, b_{k-1})$, the predicted PDF $p_+(\boldsymbol{\zeta}|\boldsymbol{z}_{1:k-1})$ under the transition density of (21) is still an NNIWGG form given by

$$p_+(\boldsymbol{\zeta}|\boldsymbol{z}_{1:k-1}) = \text{NNIWGG}(\boldsymbol{\zeta}'; \phi_{k|k-1}) \tag{23}$$

with $\phi_{k|k-1} = (\boldsymbol{m}_{k|k-1}, \boldsymbol{P}_{k|k-1}, \boldsymbol{\eta}_{k|k-1}, \beta_{k|k-1}, t_{k|k-1}, \boldsymbol{T}_{k|k-1}, a_{k|k-1}, b_{k|k-1})$ and the parameters are calculated by (9)-(13).

Since it is challenging to obtain an analytical solution for the joint posterior PDF $p(\boldsymbol{\zeta}|\boldsymbol{z}_{1:k})$ as shown in (20), hence, an approximate PDF can be achieved by the VB approach. An approximate solution of the joint posterior PDF $p(\boldsymbol{\zeta}|\boldsymbol{z}_{1:k})$ can be given by Lemma 2.

Lemma 2: According to the mean field theory [39], the joint posterior PDF $p(\boldsymbol{\zeta}|\boldsymbol{z}_{1:k})$ can be factorized as

$$p(\boldsymbol{\zeta}|\boldsymbol{z}_{1:k}) \approx q(\boldsymbol{x})q(\boldsymbol{\mu}, \boldsymbol{R})q(\lambda)q(v) \tag{24}$$

with

$$q(\boldsymbol{x}) = \text{N}(\boldsymbol{x}; \boldsymbol{m}_k, \boldsymbol{P}_k) \tag{25}$$
$$q(\boldsymbol{\mu}, \boldsymbol{R}) = \text{N}(\boldsymbol{\mu}; \boldsymbol{\eta}_k, \beta_k\boldsymbol{R})\text{IW}(\boldsymbol{R}; t_k, \boldsymbol{T}_k) \tag{26}$$
$$q(\lambda) = \text{G}(\lambda; v/2, v/2) \tag{27}$$
$$q(v) = \text{G}(v; a_k, b_k) \tag{28}$$

and given the initial value for each variational parameter as follows $t_k^{(0)} = t_{k|k-1} + 1$, $\boldsymbol{T}_k^{(0)} = \boldsymbol{T}_{k|k-1}$, $a_k^{(0)} = a_{k|k-1} + 0.5$, $b_k^{(0)} = b_{k|k-1}$, $\boldsymbol{\eta}_k^{(0)} = \boldsymbol{\eta}_{k|k-1}$, $\beta_k^{(j)} = \beta_{k|k-1}$, $c_k^{(0)} = d_k^{(0)} = 0.5a_{k|k-1}/b_{k|k-1}$, $\text{E}^{(0)}[\boldsymbol{\mu}] = \boldsymbol{\eta}_{k|k-1}$, $\text{E}^{(0)}[\boldsymbol{R}^{-1}] = t_k^{(0)}\left\{\boldsymbol{T}_k^{(0)}\right\}^{-1}$, $\text{E}^{(0)}[\lambda] = c_k^{(0)}/d_k^{(0)}$, $\text{E}^{(0)}[v] = a_k^{(0)}/b_k^{(0)}$, the parameters $\boldsymbol{m}_k$,$\boldsymbol{P}_k$,$\boldsymbol{\eta}_k$,β_k,t_k,$\boldsymbol{T}_k$,a_k,b_k can be calculated by performing the following iterative procedure, where the j-th iteration is given by

$$\tilde{\boldsymbol{R}}_k^{(j)} = \frac{\{\text{E}^{(j-1)}[\boldsymbol{R}^{-1}]\}^{-1}}{\text{E}^{(j-1)}[\lambda]} \tag{29}$$
$$\boldsymbol{K}_k^{(j)} = \boldsymbol{P}_{k|k-1}\boldsymbol{H}^{\text{T}}\left(\boldsymbol{H}\boldsymbol{P}_{k|k-1}\boldsymbol{H}^{\text{T}} + \tilde{\boldsymbol{R}}_k^{(j)}\right)^{-1} \tag{30}$$
$$\boldsymbol{m}_k^{(j)} = \boldsymbol{m}_{k|k-1} + \boldsymbol{K}_k^{(j)}(\boldsymbol{z}_k - \boldsymbol{H}\boldsymbol{m}_{k|k-1} - \text{E}^{(j-1)}[\boldsymbol{\mu}]) \tag{31}$$
$$\boldsymbol{P}_k^{(j)} = (\boldsymbol{I}_n - \boldsymbol{K}_k^{(j)}\boldsymbol{H})\boldsymbol{P}_{k|k-1} \tag{32}$$
$$\boldsymbol{\eta}_k^{(j)} = \boldsymbol{\eta}_{k|k-1} + \boldsymbol{W}_k^{(j)}(\tilde{\boldsymbol{z}}_k^{(j)} - \boldsymbol{\mu}_{k|k-1}) \tag{33}$$
$$\beta_k^{(j)} = \frac{\beta_{k|k-1}}{1 + \beta_{k|k-1}\text{E}^{(j-1)}[\lambda]} \tag{34}$$
$$\boldsymbol{W}_k^{(j)} = \left(1 - \frac{1}{1 + \beta_{k|k-1}\text{E}^{(j-1)}[\lambda]}\right)\boldsymbol{I}_m \tag{35}$$
$$\tilde{\boldsymbol{z}}_k^{(j)} = \boldsymbol{z}_k - \boldsymbol{H}\boldsymbol{m}_k^{(j)} \tag{36}$$
$$t_k^{(j)} = t_{k|k-1} + 1 \tag{37}$$
$$\boldsymbol{T}_k^{(j)} = \boldsymbol{T}_{k|k-1} + \text{E}^{(j-1)}[\lambda]\boldsymbol{A}_k^{(j-1)} \tag{38}$$
$$\boldsymbol{A}_k^{(j-1)} = \boldsymbol{H}\boldsymbol{P}_k^{(j)}\boldsymbol{H}^{\text{T}} + \frac{[\tilde{\boldsymbol{z}}_k^{(j)} - \boldsymbol{\eta}_{k|k-1}][\tilde{\boldsymbol{z}}_k^{(j)} - \boldsymbol{\eta}_{k|k-1}]^{\text{T}}}{\beta_{k|k-1}\text{E}^{(j-1)}[\lambda] + 1} \tag{39}$$
$$c_k^{(j)} = \frac{\text{E}^{(j-1)}[v] + m}{2} \tag{40}$$
$$d_k^{(j)} = \frac{\text{E}^{(j-1)}[v] + tr\left(\boldsymbol{B}_k^{(j)}\text{E}^{(j)}[\boldsymbol{R}^{-1}]\right)}{2} \tag{41}$$
$$\boldsymbol{B}_k^{(j)} = (\tilde{\boldsymbol{z}}_k^{(j)} - \boldsymbol{\eta}_k^{(j)})(\tilde{\boldsymbol{z}}_k^{(j)} - \boldsymbol{\eta}_k^{(j)})^{\text{T}} + \boldsymbol{H}\boldsymbol{P}_k^{(j)}\boldsymbol{H}^{\text{T}} + \boldsymbol{P}_{\boldsymbol{\mu}}^{(j)} \tag{42}$$
$$\boldsymbol{P}_{\boldsymbol{\mu}}^{(j)} = \beta_k^{(j)}\boldsymbol{T}_k^{(j)}/t_k^{(j)} \tag{43}$$
$$\boldsymbol{C}_k^{(j)} = \boldsymbol{P}_k^{(j)} + (\boldsymbol{m}_k^{(j)} - \boldsymbol{m}_{k|k-1})(\boldsymbol{m}_k^{(j)} - \boldsymbol{m}_{k|k-1})^{\text{T}} \tag{44}$$
$$\boldsymbol{D}_k^{(j)} = (\boldsymbol{\eta}_k^{(j)} - \boldsymbol{\eta}_{k|k-1})(\boldsymbol{\eta}_k^{(j)} - \boldsymbol{\eta}_{k|k-1})^{\text{T}} + \boldsymbol{P}_{\boldsymbol{\mu}}^{(j)} \tag{45}$$
$$a_k^{(j)} = a_{k|k-1} + 0.5 \tag{46}$$
$$b_k^{(j)} = b_{k|k-1} - 0.5 - 0.5\text{E}^{(j)}[\ln\lambda] + 0.5\text{E}^{(j)}[\lambda] \tag{47}$$
$$\text{E}^{(j)}[\boldsymbol{\mu}] = \boldsymbol{\eta}_k^{(j)} \tag{48}$$
$$\text{E}^{(j)}[\boldsymbol{R}^{-1}] = t_k^{(j)}\left\{\boldsymbol{T}_k^{(j)}\right\}^{-1} \tag{49}$$
$$\text{E}^{(j)}[\lambda] = c_k^{(j)}/d_k^{(j)} \tag{50}$$
$$\text{E}^{(j)}[\ln\lambda] = \psi(c_k^{(j)}) - \ln(d_k^{(j)}) \tag{51}$$
$$\text{E}^{(j)}[v] = a_k^{(j)}/b_k^{(j)} \tag{52}$$
$$\text{E}^{(j)}[\ln v] = \psi(a_k^{(j)}) - \ln(b_k^{(j)}) \tag{53}$$

where $\psi(\cdot)$ is the digamma function [27], the required expectations as shown in (48)-(53) can be calculated from (26)-(28) respectively.

The iterative procedure is terminated when the following convergence conditions are satisfied

$$\frac{\left\|\boldsymbol{m}_k^{(j)} - \boldsymbol{m}_k^{(j-1)}\right\|_2}{\left\|\boldsymbol{m}_k^{(j)}\right\|_2} \le \tau \text{ or } j > N_{\max}, \quad j \in 1, 2, \ldots, N_{\max} \tag{54}$$

where τ denotes an iteration threshold, $N_{\max}$ is the maximum iteration number, and $\|\boldsymbol{M}\|_2$ means the 2-Norm of vector $\boldsymbol{M}$. If (54) holds, the j-th iteration of each parameter is substituted into (25)-(28) respectively, and the final approximate posterior densities can be obtained.

The Lemma 2 is proved in Appendix A.

Using the Corollary 1 in [32], the following relation holds

$$\text{N}(\boldsymbol{z}_k; \boldsymbol{H}\boldsymbol{x} + \boldsymbol{\mu}, \boldsymbol{R}/\lambda)\text{NNIWGG}(\boldsymbol{\zeta}; \phi_{k|k-1}) \approx q(\boldsymbol{z}_k)\text{NNIWGG}(\boldsymbol{\zeta}; \phi_k) \tag{55}$$

where $q(z_k)$ is the variational lower bound calculated as in (54).

It can be obtained by substituting (9)-(13) and (29)-(53), which satisfies the convergence condition into (56). For ease of description, the exponential term is derived from the subtraction of two parts.

$$q(z_k) = \exp\{L_1 - L_2\} \tag{56}$$

where the first part L_1 in the exponential term of (56) is given by

$$\begin{aligned} L_1 = & -\frac{2m+n}{2}\ln(2\pi) + \frac{m}{2}\mathrm{E}[\ln\lambda] - \frac{1}{2}\mathrm{tr}\left(\mathrm{E}[\lambda]\mathrm{E}[\boldsymbol{R}^{-1}]\boldsymbol{B}_k\right) \\ & -\frac{1}{2}\ln|\boldsymbol{P}_{k|k-1}| - \frac{1}{2}\mathrm{tr}\left(\boldsymbol{P}_{k|k-1}^{-1}\boldsymbol{C}_k\right) - \frac{m}{2}\ln\beta_{k|k-1} \\ & -\frac{1}{2}\mathrm{tr}\left(\frac{\mathrm{E}[\boldsymbol{R}^{-1}]}{\beta_{k|k-1}}\boldsymbol{D}_k\right) + \frac{t_{k|k-1}}{2}\ln|\boldsymbol{T}_{k|k-1}| \\ & -\frac{m+1}{2}t_{k|k-1}\ln 2 - \ln\Gamma\left(\frac{t_{k|k-1}}{2}\right) \\ & -\frac{m+t_{k|k-1}+3}{2}\mathrm{E}[\ln|\boldsymbol{R}|] - \frac{1}{2}\mathrm{tr}\left(\mathrm{E}[\boldsymbol{R}^{-1}]\boldsymbol{T}_{k|k-1}\right) \\ & +\frac{1}{2}\mathrm{E}[\ln v] + \frac{1}{2}\mathrm{E}[v] + \left(\frac{1}{2}\mathrm{E}[v]-1\right)\mathrm{E}[\ln\lambda] \\ & -\frac{1}{2}\mathrm{E}[v]\mathrm{E}[\lambda] + a_{k|k-1}\ln b_{k|k-1} - \ln\Gamma(a_{k|k-1}) \\ & +(a_{k|k-1}-1)\mathrm{E}[\ln v] - b_{k|k-1}\mathrm{E}[v] \end{aligned} \tag{57}$$

while the second part L_2 can be calculated as follows

$$\begin{aligned} L_2 = & -\frac{m+n}{2}\ln(2\pi) - \frac{1}{2}\ln|\boldsymbol{P}_k| - \frac{n}{2} - \frac{m}{2}\ln\beta_k \\ & -\frac{m}{2} + \frac{t_k}{2}\ln|\boldsymbol{T}_k| - \frac{m}{2}t_k\ln 2 - \ln\Gamma\left(\frac{t_k}{2}\right) \\ & -\frac{m+t_k+2}{2}\mathrm{E}[\ln|\boldsymbol{R}|] - \frac{1}{2}\mathrm{tr}\left(\mathrm{E}[\boldsymbol{R}^{-1}]\boldsymbol{T}_k\right) \\ & +c_k\ln d_k - \ln\Gamma(c_k) + (c_k-1)\mathrm{E}[\ln\lambda] - d_k\mathrm{E}[\lambda] \\ & +a_k\ln b_k - \ln\Gamma(a_k) + (a_k-1)\mathrm{E}[\ln v] - b_k\mathrm{E}[v]. \end{aligned} \tag{58}$$

The derivation of $q(z_k)$ is given in Appendix B.

B. THE ROBUST J-GLMB FILTER

To carry out MTT under unknown non-stationary HTMN, the VB approach is introduced into the J-GLMB filtering framework, and then the robust J-GLMB filter which can jointly estimate the unknown parameters in the augmented state is proposed. From the point of view of Bayesian filtering, the key of the proposed algorithm is to recursively estimate the joint posterior multitarget density $p^{(\xi)}(\boldsymbol{\zeta}, \ell)$ with the augmented state. Then, the multitarget state of the robust J-GLMB filter is extended to a hybrid state space $\boldsymbol{\Lambda} = \{(\boldsymbol{\zeta}, \ell)_i\}(i = 1, 2, \ldots, N)$, where N is the number of target states. The multitarget measurement can be modeled as RFS, $\boldsymbol{Z} = \{\boldsymbol{z}_1, \boldsymbol{z}_2, \ldots, \boldsymbol{z}_{|\boldsymbol{Z}|}\}$, where $\boldsymbol{z}_1, \ldots, \boldsymbol{z}_{|\boldsymbol{Z}|}$ denote observations of individual measurements and $|\cdot|$ is the cardinality of a collection. The joint recursion between the components of two GLMB filtering densities is provided by Proposition 1.

Proposition 1: If the joint posterior multitarget density at time k is a GLMB of the following form

$$\pi(\boldsymbol{\Lambda}) = \Delta(\boldsymbol{\Lambda})\sum_{I,\xi}\omega^{(I,\xi)}\delta_I[\mathcal{L}(\boldsymbol{\Lambda})]\left[p^{(\xi)}\right]^{\boldsymbol{\Lambda}} \tag{59}$$

where $I \in \mathcal{F}(\mathbb{L})$, $\xi \in \boldsymbol{\Xi}$, then the joint posterior multitarget density at time $k+1$ is still a GLMB of the form

$$\pi_{\boldsymbol{Z}_+}(\boldsymbol{\Lambda}) \propto \Delta(\boldsymbol{\Lambda})\sum_{I,\xi,I_+,\theta_+}\omega^{(I,\xi)}\omega_{\boldsymbol{Z}_+}^{(I,\xi,I_+,\theta_+)}\delta_{I_+}[\mathcal{L}(\boldsymbol{\Lambda})]\left[p_{\boldsymbol{Z}_+}^{(\xi,\theta_+)}\right]^{\boldsymbol{\Lambda}} \tag{60}$$

where $I_+ \in \mathcal{F}(\mathbb{L}_+)$, $\theta_+ \in \boldsymbol{\Theta}_+$, and

$$\begin{aligned} & \omega_{\boldsymbol{Z}_+}^{(I,\xi,I_+,\theta_+)} \\ & = 1_{\boldsymbol{\Theta}_+(I_+)}(\theta_+)\left[1-\bar{P}_S^{(\xi)}\right]^{I-I_+}\left[\bar{P}_S^{(\xi)}\right]^{I\bigcap I_+} \\ & \quad \times[1-r_{B,+}]^{\mathbb{B}_+-I_+}r_{B,+}^{\mathbb{B}_+\bigcap I_+}\left[\bar{\psi}_{\boldsymbol{Z}_+}^{(\xi,\theta_+)}\right]^{I_+} \end{aligned} \tag{61}$$

$$p_{\boldsymbol{Z}_+}^{(\xi,\theta_+)}(\boldsymbol{\zeta}_+, \ell_+) = \frac{\bar{p}_+^{(\xi)}(\boldsymbol{\zeta}_+, \ell_+)\psi_{\boldsymbol{Z}_+}^{(\theta_+(\ell_+))}(\boldsymbol{\zeta}_+, \ell_+)}{\bar{\psi}_{\boldsymbol{Z}_+}^{(\xi,\theta_+)}(\ell_+)} \tag{62}$$

$$\begin{aligned} & \bar{p}_+^{(\xi)}(\boldsymbol{\zeta}_+, \ell_+) \\ & = 1_{\mathbb{L}}(\ell_+)\frac{\left\langle P_S(\boldsymbol{\zeta}, \ell_+)f_+(\boldsymbol{\zeta}_+|\boldsymbol{\zeta}, \ell_+), p^{(\xi)}(\boldsymbol{\zeta}, \ell_+)\right\rangle}{\bar{P}_S^{(\xi)}(\ell_+)} \\ & \quad +1_{\mathbb{B}_+}(\ell_+)p_{B,+}(\boldsymbol{\zeta}_+, \ell_+) \end{aligned} \tag{63}$$

$$\bar{\psi}_{\boldsymbol{Z}_+}^{(\xi,\theta_+)}(\ell_+) = \left\langle \bar{p}_+^{(\xi)}(\boldsymbol{\zeta}_+, \ell_+), \psi_{\boldsymbol{Z}_+}^{(\theta_+(\ell_+))}(\boldsymbol{\zeta}_+, \ell_+)\right\rangle \tag{64}$$

$$\bar{P}_S^{(\xi)}(\ell) = \left\langle p^{(\xi)}(\boldsymbol{\zeta}, \ell), P_S(\boldsymbol{\zeta}, \ell)\right\rangle \tag{65}$$

$$\begin{aligned} & \psi_{\boldsymbol{Z}_+}^{(\theta_+(\ell_+))}(\boldsymbol{\zeta}_+, \ell_+) \\ & = \begin{cases} \dfrac{P_D(\boldsymbol{\zeta}_+, \ell)g(\boldsymbol{z}_{\theta_+(\ell_+)}|\boldsymbol{\zeta}_+, \ell_+)}{\kappa(\boldsymbol{z}_{\theta_+(\ell_+)})}, & \theta_+(\ell_+) = \{1, \ldots, |\boldsymbol{Z}_+|\} \\ 1-P_D(\boldsymbol{\zeta}_+, \ell), & \theta_+(\ell_+) = 0 \end{cases} \end{aligned} \tag{66}$$

where $\boldsymbol{Z}_+ = \{\boldsymbol{z}_{1:|\boldsymbol{Z}_+|}\}$ denotes the multitarget measurement RFS at time $k+1$ from detected targets, and $P_S(\boldsymbol{\zeta}, \ell)$ and $P_D(\boldsymbol{\zeta}_+, \ell)$ represent the survival probability and the detection probability respectively,$f_+(\boldsymbol{\zeta}_+|\boldsymbol{\zeta}, \ell_+)$ is the single target Markov transition kernel, $g(\boldsymbol{z}_{\theta_+(\ell_+)}|\boldsymbol{\zeta}_+, \ell_+)$ is the single target likelihood for $\boldsymbol{z}_{\theta_+(\ell_+)}$ given $(\boldsymbol{\zeta}_+, \ell_+)$, and $\kappa(\boldsymbol{z}_{\boldsymbol{\theta}_+(\ell_+)})$ is the clutter density function. In addition, the label space for new targets is $\mathbb{B}_+$, $r_{B,+}(\ell_+)$ is probability that a new object with label ℓ_+ is born, and $p_{B,+}(x_+, \ell_+)$ is the distribution of its kinematic state.

C. CALCULATION OF PARAMETERS

To obtain a closed-form formula of the robust J-GLMB filter, the following assumptions are given.

Assumption 1: Suppose that each target follows the NNIWGG model as (21) and the measurement model as (5).

Assumption 2: The survival probability and detection probability are independent of the augmented state and label, that is,

$$P_S(\boldsymbol{\zeta}, \ell) = P_S \tag{67}$$
$$P_D(\boldsymbol{\zeta}, \ell) = P_D. \tag{68}$$

Assumption 3: Suppose that the target birth model has the same form, namely that of an LMB distribution at every time step, and the target birth intensity can be represented as an NNIWGG form

$$p_{B,+}(\boldsymbol{\zeta}, \ell) = \sum_{j=1}^{J_B(\ell)} w_B^{(j)}(\ell)\text{NNIWGG}(\boldsymbol{\zeta}; \boldsymbol{\phi}_B^{(j)}(\ell)) \tag{69}$$

where $\boldsymbol{\phi}_B^{(j)}(\ell) = (\boldsymbol{m}_B^{(j)}(\ell), \boldsymbol{P}_B^{(j)}(\ell), \boldsymbol{\eta}_B^{(j)}(\ell), \beta_B^{(j)}(\ell), t_B^{(j)}(\ell), \boldsymbol{T}_B^{(j)}(\ell), a_B^{(j)}(\ell), b_B^{(j)}(\ell))$, $J_B(\ell)$, and $w_B^{(j)}(\ell)$ are the given model parameters that determine the shape of the birth intensity.

Based on the above assumptions, Lemma 1, and Lemma 2, the GLMB component parameters can be calculated by Proposition 2. For the sake of simplicity and compactness, the labels ℓ and ℓ_+ are omitted.

Proposition 2: Suppose the joint posterior multitarget density is shown in (59), where the single target density is the NNIWGG form

$$p^{(\xi)}(\boldsymbol{\zeta}) = \sum_{i=1}^{J^{(\xi)}} w_{k-1}^{(\xi,i)}\text{NNIWGG}(\boldsymbol{\zeta}; \phi_{k-1}^{(\xi,i)}) \tag{70}$$

where $\phi_{k-1}^{(\xi,i)} = (\boldsymbol{m}_{k-1}^{(\xi,i)}, \boldsymbol{P}_{k-1}^{(\xi,i)}, \boldsymbol{\eta}_{k-1}^{(\xi,i)}, \beta_{k-1}^{(\xi,i)}, t_{k-1}^{(\xi,i)}, \boldsymbol{T}_{k-1}^{(\xi,i)}, a_{k-1}^{(\xi,i)}, b_{k-1}^{(\xi,i)})$, then the single target predicted density $\bar{p}_+^{(\xi)}(\boldsymbol{\zeta}_+)$ can be obtained

$$\bar{p}_+^{(\xi)}(\boldsymbol{\zeta}_+) = 1_{\mathbb{L}}(\ell_+)\sum_{i=1}^{J^{(\xi)}} w_{S,k|k-1}^{(\xi,i)}\text{NNIWGG}(\boldsymbol{\zeta}_+; \boldsymbol{\phi}_{S,k|k-1}^{(\xi,i)}) + 1_{\mathbb{B}_+}(\ell_+)p_{B,+}(\boldsymbol{\zeta}_+) \tag{71}$$

where $\boldsymbol{\phi}_{S,k|k-1}^{(\xi,i)} = (\boldsymbol{m}_{S,k|k-1}^{(\xi,i)}, \boldsymbol{P}_{S,k|k-1}^{(\xi,i)}, \boldsymbol{\eta}_{S,k|k-1}^{(\xi,i)}, \beta_{S,k|k-1}^{(\xi,i)}, t_{S,k|k-1}^{(\xi,i)}, \boldsymbol{T}_{S,k|k-1}^{(\xi,i)}, a_{S,k|k-1}^{(\xi,i)}, b_{S,k|k-1}^{(\xi,i)})$, in which each parameter can be computed by Lemma 1.

Proof: Substituting (32), (65), (67) and (70) into the first term on the right-hand side of (63), and exchanging the order of integral and summation, and using Lemma 1 to obtain the first term on the right-hand side of (71), while the second term on the right-hand side of (63) is shown in (69).

Proposition 3: Suppose that the predicted single target density $\bar{p}_+^{(\xi)}(\boldsymbol{\zeta}_+)$ at time k can be represented as the following NNIWGG form

$$\bar{p}_+^{(\xi)}(\boldsymbol{\zeta}_+) = \sum_{i=1}^{J_+^{(\xi)}} w_{k|k-1}^{(\xi,i)}\text{NNIWGG}(\boldsymbol{\zeta}; \boldsymbol{\phi}_{k|k-1}^{(\xi,i)}) \tag{72}$$

where $\boldsymbol{\phi}_{k|k-1}^{(\xi,i)} = (\boldsymbol{m}_{k|k-1}^{(\xi,i)}, \boldsymbol{P}_{k|k-1}^{(\xi,i)}, \boldsymbol{\eta}_{k|k-1}^{(\xi,i)}, \beta_{k|k-1}^{(\xi,i)}, t_{k|k-1}^{(\xi,i)}, \boldsymbol{T}_{k|k-1}^{(\xi,i)}, a_{k|k-1}^{(\xi,i)}, b_{k|k-1}^{(\xi,i)})$, then the posterior single target density $p_{\boldsymbol{Z}_+}^{(\xi,\theta_+)}(\boldsymbol{\zeta}_+)$ in (60) can also be formulated as the NNIWGG form

$$p_{\boldsymbol{Z}_+}^{(\xi,\theta_+)}(\boldsymbol{\zeta}_+) = \frac{1}{\bar{\psi}_{\boldsymbol{Z}_+}^{(\xi,\theta_+)}}\sum_{i=1}^{J_+^{(\xi)}} w_{\boldsymbol{Z}_+,i}^{(\xi,\theta_+)}\text{NNIWGG}(\boldsymbol{\zeta}_+; \boldsymbol{\phi}_{\boldsymbol{Z}_+,i}^{(\xi,\theta_+)}) \tag{73}$$

where $\boldsymbol{\phi}_{\boldsymbol{Z}_+,i}^{(\xi,\theta_+)} = (\boldsymbol{m}_{\boldsymbol{Z}_+,i}^{(\xi,\theta_+)}, \boldsymbol{P}_{\boldsymbol{Z}_+,i}^{(\xi,\theta_+)}, \boldsymbol{\eta}_{\boldsymbol{Z}_+,i}^{(\xi,\theta_+)}, \beta_{\boldsymbol{Z}_+,i}^{(\xi,\theta_+)}, t_{\boldsymbol{Z}_+,i}^{(\xi,\theta_+)}, \boldsymbol{T}_{\boldsymbol{Z}_+,i}^{(\xi,\theta_+)}, a_{\boldsymbol{Z}_+,i}^{(\xi,\theta_+)}, b_{\boldsymbol{Z}_+,i}^{(\xi,\theta_+)})$, and the normalization constant is given by

$$\bar{\psi}_{\boldsymbol{Z}_+}^{(\xi,\theta_+)} = \sum_{i=1}^{J_+^{(\xi)}} w_{\boldsymbol{Z}_+,i}^{(\xi,\theta_+)} \tag{74}$$

For $\theta_+(\ell_+) = 0$, we have

$$w_{\boldsymbol{Z}_+,i}^{(\xi,\theta_+)} = w_{k|k-1}^{(\xi,i)}(1 - P_D) \tag{75}$$
$$\boldsymbol{m}_{\boldsymbol{Z}_+,i}^{(\xi,\theta_+)} = \boldsymbol{m}_{k|k-1}^{(\xi,i)}, \boldsymbol{P}_{\boldsymbol{Z}_+,i}^{(\xi,\theta_+)} = \boldsymbol{P}_{k|k-1}^{(\xi,i)} \tag{76}$$
$$\boldsymbol{\eta}_{\boldsymbol{Z}_+,i}^{(\xi,\theta_+)} = \boldsymbol{\eta}_{k|k-1}^{(\xi,i)}, \beta_{\boldsymbol{Z}_+,i}^{(\xi,\theta_+)} = \beta_{k|k-1}^{(\xi,i)} \tag{77}$$
$$t_{\boldsymbol{Z}_+,i}^{(\xi,\theta_+)} = t_{k|k-1}^{(\xi,i)}, \boldsymbol{T}_{\boldsymbol{Z}_+,i}^{(\xi,\theta_+)} = \boldsymbol{T}_{k|k-1}^{(\xi,i)} \tag{78}$$
$$a_{\boldsymbol{Z}_+,i}^{(\xi,\theta_+)} = a_{k|k-1}^{(\xi,i)}, b_{\boldsymbol{Z}_+,i}^{(\xi,\theta_+)} = b_{k|k-1}^{(\xi,i)} \tag{79}$$

If $\theta_+(\ell_+) > 0$, then

$$w_{\boldsymbol{Z}_+,i}^{(\xi,\theta_+)} = w_{k|k-1}^{(\xi,i)}\frac{q_i^{(\xi)}(\boldsymbol{z}_{\theta_+})P_D}{\kappa(\boldsymbol{z}_{\theta_+})} \tag{80}$$

where the approximate likelihood $q_i^{(\xi)}(\boldsymbol{z}_{\theta_+})$ can be calculated using $\boldsymbol{m}_{\boldsymbol{Z}_+,i}^{(\xi,\theta_+)}$, $\boldsymbol{P}_{\boldsymbol{Z}_+,i}^{(\xi,\theta_+)}$, $\boldsymbol{\eta}_{\boldsymbol{Z}_+,i}^{(\xi,\theta_+)}$, $\beta_{\boldsymbol{Z}_+,i}^{(\xi,\theta_+)}$, $t_{\boldsymbol{Z}_+,i}^{(\xi,\theta_+)}$, $\boldsymbol{T}_{\boldsymbol{Z}_+,i}^{(\xi,\theta_+)}$, $a_{\boldsymbol{Z}_+,i}^{(\xi,\theta_+)}$, and $b_{\boldsymbol{Z}_+,i}^{(\xi,\theta_+)}$ according to (56). The final values of these parameters are obtained by (29)-(53) given $\boldsymbol{\phi}_{k|k-1}^{(\xi,i)}$.

IV. SIMULATION RESULTS

The proposed NNIWGG-J-GLMB filter is compared with the existing NGIWG-LMB filter [32], STM-LMB filter [33] and GM-J-GLMB filter [10]. Both the optimal sub-pattern assignment (OSPA) [40] and OSPA$^{(2)}$ (OSPA-on-OSPA) [18], [41] distances are utilized to evaluate the performance of all four filters. For the OSPA distance, the cut-off parameter is $c = 100$m, the order parameter is $p = 1$, and for the OSPA$^{(2)}$ distance, the window length is set to $L_w = 10$. Note that the OSPA$^{(2)}$ distance not only accounts for errors in both localization and cardinality, but also captures track labeling errors. Therefore, the OSPA$^{(2)}$ distance is more rigorous, and it is particularly suitable to be applied to evaluate the performance of the labeled RFS filters. In particular, the OSPA$^{(2)}$ distance reduces to OSPA distance when $L_w = 1$, that is, the OSPA distance is a special form of the OSPA$^{(2)}$ distance.

A. LINEAR SCENARIOS

The linear MTT scenarios are the same as that in [32]. The single target state is given by $\boldsymbol{x}_k = [p_{x,k}, \dot{p}_{x,k}, p_{y,k}, \dot{p}_{y,k}]$ which contains position vector $(p_{x,k}, p_{y,k})$ and velocity vector $(\dot{p}_{x,k}, \dot{p}_{y,k})$. Each target follows a linear Gaussian

model with the Markov transition density $f(\boldsymbol{x}_k|\boldsymbol{x}_{k-1}) = N(\boldsymbol{x}_k; \boldsymbol{F}\boldsymbol{x}_{k-1}, \boldsymbol{Q}_{k-1})$, where $\boldsymbol{F} = \boldsymbol{I}_2 \otimes \begin{bmatrix} 1 & T \\ 0 & 1 \end{bmatrix}$, $\boldsymbol{Q}_{k-1} = \sigma_w^2 \begin{bmatrix} T^4/4 & T^3/3 \\ T^3/3 & T^2 \end{bmatrix} \otimes \boldsymbol{I}_2$, and the sampling interval $T = 1$s, the standard deviation of the process noise is $\sigma_w = 5\text{m/s}^2$, the identity matrix of dimension $n \times n$ is denoted by $\boldsymbol{I}_n$, and $\otimes$ is the Kronecker product between two matrices of arbitrary size.

The measurement model with unknown non-stationary HTMN is formulated as

$$\boldsymbol{z}_k = \begin{bmatrix} 1 & 0 & 0 & 0 \\ 0 & 0 & 1 & 0 \end{bmatrix} \boldsymbol{x}_k + \boldsymbol{\varepsilon}_k. \tag{81}$$

The unknown non-stationary HTMN $\boldsymbol{\varepsilon}_k$ is generated as follows [35]

$$\boldsymbol{\varepsilon}_k \sim \begin{cases} \mathrm{N}(\boldsymbol{\eta}_k, \boldsymbol{R}_0) & \text{with probability } -P_g \\ \mathrm{N}(\boldsymbol{\eta}_k, 100\boldsymbol{R}_0) & \text{with probability } P_g \end{cases} \tag{82}$$

where P_g is the probability of non-stationary HTMN outliers, and $\boldsymbol{R}_0 = \mathrm{diag}([100\text{m}^2, 100\text{m}^2])$ is a nominal variance matrix, the true mean vector is given by

$$\boldsymbol{\eta}_k = \begin{cases} [10\text{m}; 10\text{m}] & k \in (0, 25\text{s}] \\ [20\text{m}; 20\text{m}] & k \in (25\text{s}, 50\text{s}] \\ [30\text{m}; 30\text{m}] & k \in (50\text{s}, 75\text{s}] \\ [10\text{m}; 10\text{m}] & k \in (75\text{s}, 100\text{s}] \end{cases} \tag{83}$$

It should be noted that this model reduces to the stationary HTMN as shown in [32] when $\boldsymbol{\eta}_k = [0; 0]$.

The clutter is modeled as a Poisson RFS with the intensity function $\kappa(z) = \lambda_c V u(z)$, where λ_c is the expected number of false alarms per scan, V and $u(\cdot)$ represent the volume of the surveillance region and the uniform density, respectively. Further, the survival probability is given by $P_S = 0.99$, and the detection probability P_D and the average number of clutter λ_c are separately specified by different simulation experiments.

The birth targets are modeled as an LMB RFS with parameters $\pi_B = \{r_B, p_B^{(i)}(\boldsymbol{\zeta})\}_{i=1}^4$, where the existence probabilities $r_B = 0.03$, and the spatial distribution of the birth targets follows an NNIWGG model

$$p_B^{(i)}(\boldsymbol{\zeta}) = \mathrm{NNIWGG}(\boldsymbol{\zeta}; \boldsymbol{\phi}_B^{(i)}) \tag{84}$$

where $\boldsymbol{\phi}_B^{(i)} = (\boldsymbol{m}_B^{(i)}, \boldsymbol{P}_B, \boldsymbol{\eta}_B, \beta_B, t_B, \boldsymbol{T}_B, a_B, b_B)$ with $\boldsymbol{m}_B^{(1)} = [0.1,0,0.1,0]^{\mathrm{T}}$, $\boldsymbol{m}_B^{(2)} = [400,0,-600,0]^{\mathrm{T}}$, $\boldsymbol{m}_B^{(3)} = [-800,0,-200,0]^{\mathrm{T}}$, $\boldsymbol{m}_B^{(4)} = [-200,0,800,0]^{\mathrm{T}}$, $\boldsymbol{P}_B = \mathrm{diag}([10^2, 10^2, 10^2, 10^2])$, while $\boldsymbol{\eta}_B = [0; 0]$, $\beta_B = 1$, $t_B = 5$, $\boldsymbol{T}_B = \mathrm{diag}([10^2, 10^2])$, $a_B = 5$, $b_B = 1$. In addition, the mixture terms for each hypothesized track are pruned and merged with a pruning threshold of $T_m = 10^{-5}$, a merging threshold $U_m = 4$ m, and a maximum number of mixture terms $J_{\max} = 100$. Moreover, the hypotheses are pruned with a pruning threshold of $T_h = 10^{-4}$ and the maximum number of GLMB components is capped at $H_{\max} = 10^3$.

Fig. 1 gives the true trajectories, measurements and state estimates of a single trial obtained by the four filters with $P_g = 0.10$, $P_D = 0.95$, $\lambda_c = 20$, $\rho = 0.90$, and $N_{\max} = 5$. It is shown that the proposed NNIWGG-J-GLMB filter achieves satisfactory tracking results. However, the other three filters have lost part of the target trajectories, among which the trajectories loss of the GM-J-GLMB filter is the most serious. The simulation results indicate that the proposed filter can provide the best tracking accuracy in almost all the time. These results are reasonable, since the measurement noise is approximated by a Student's t-distribution with unknown and time-varying mean.

As described in Fig. 2, the estimated cardinality for these filters with $P_g = 0.10$, $P_D = 0.95$, $\lambda_c = 20$, $\rho = 0.90$, and $N_{\max} = 5$ averaged over 100 Monte Carlo (MC) trials. It is apparent that the four filters can provide unbiased cardinality estimates at the beginning of the tracking, however, the cardinality estimates of the other three filters except the proposed NNIWGG-J-GLMB filter are underestimated because of the trajectories loss. As expected, the proposed filter can correctly estimate the number of targets in the whole tracking period. This mainly because the proposed filter is robust to the HTMN and adaptive to non-stationary noise.

Fig. 3a and Fig. 3b respectively show the average OSPA and OSPA$^{(2)}$ distances over 100 MC trials. Obviously, the proposed filter has the smallest OSPA and OSPA$^{(2)}$ distances for almost all the time. As shown in Fig. 3a, when targets appear and disappear, the OSPA distances of the four filters yield significant peaks. Fig. 3b shows the GM-J-GLMB filter has the smallest OSPA$^{(2)}$ distance in the initial period, while after 25s, the proposed filter can achieve the best performance. There are two main reasons: firstly, in the initial 25s, the deviation from zero-mean is relatively small, and secondly, both the NGIWG-LMB filter and the proposed filter need to learn the noise parameters online via the VB approach, hence their corresponding tracking accuracies may not be ideal at this initial stage. However, the OSPA$^{(2)}$ distance of both the NGIWG-LMB filter and the proposed filter are smaller than that of the GM-J-GLMB filter and STM-LMB filter with the change of the mean of non-stationary HTMN. It can be found that the OSPA$^{(2)}$ and OSPA distances have a common trend, and both of them indicate that the proposed filter has the best performance. In addition, the OSPA$^{(2)}$ distances of the four filters are significantly larger than their corresponding OSPA distances, because the OSPA$^{(2)}$ distance penalizes incorrect labelling behavior which is not considered in the OSPA distance [40].

To further verify the effectiveness of the proposed filter, the performances of the four filters are compared with different λ_c, P_D and P_g. Both of the OSPA and OSPA$^{(2)}$ distances are the average results over 100 MC trials, and the true target trajectories in each MC trial remain unchanged, but the measurements and clutter are generated randomly and independently.

Fig. 4a and Fig. 4b respectively show the average OSPA and OSPA$^{(2)}$ distances when λ_c varies from 5 to 60 with

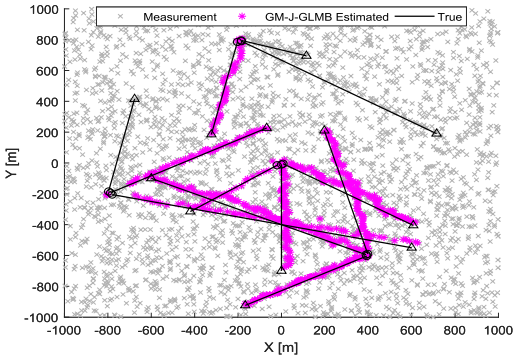

(a) GM-J-GLMB filter

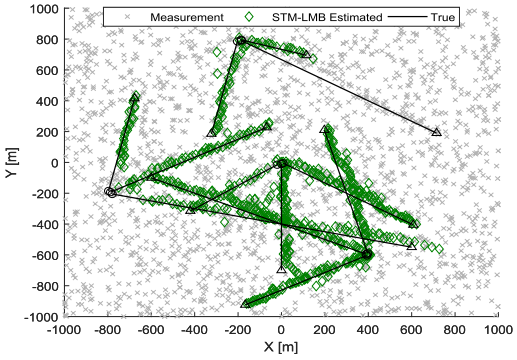

(b) STM-LMB filter

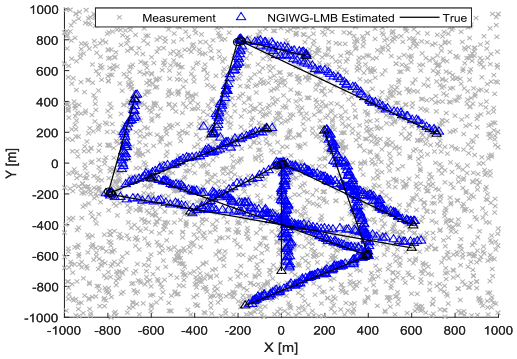

(c) NGIWG-LMB filter

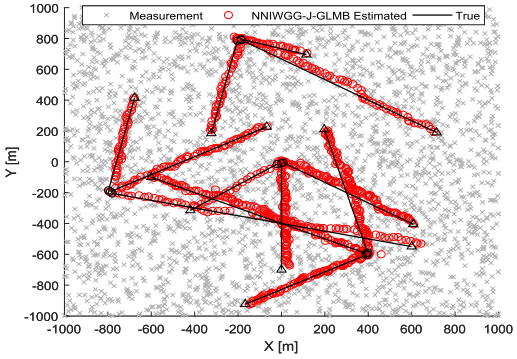

(d) NNIWGG-J-GLMB filter

FIGURE 1. The ground truth (black lines) and estimated trajectories (colored labels) of the four filters.

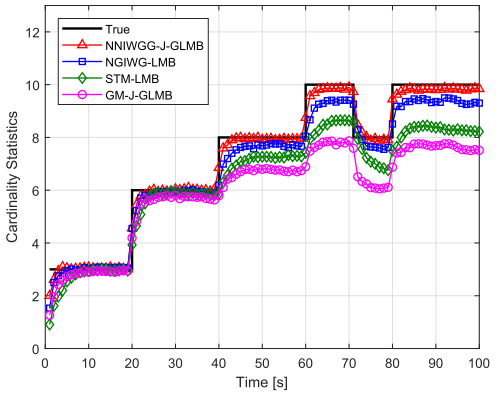

FIGURE 2. The true and estimated cardinality for the four filters over time.

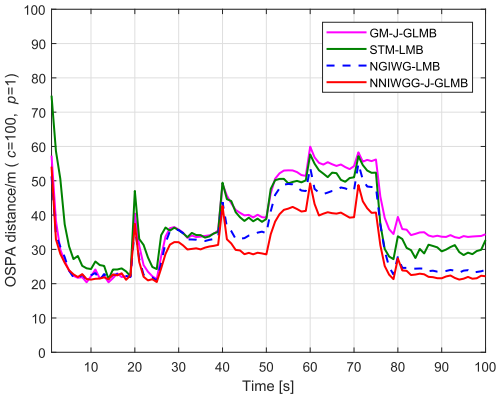

(a) OSPA distances

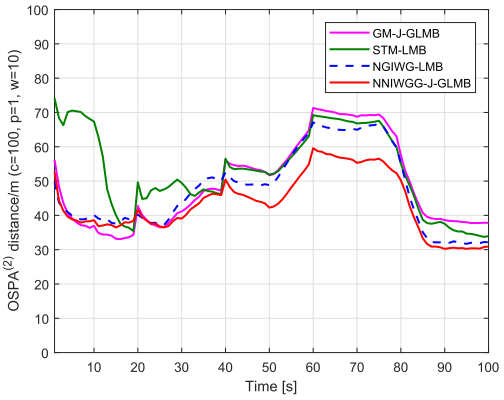

(b) OSPA$^{(2)}$ distances

FIGURE 3. OSPA and OSPA$^{(2)}$ distances for the four filters over time.

$P_g = 0.10$, $P_D = 0.95$, $\rho = 0.90$, and $N_{\max} = 5$. The simulation results indicate that the tracking accuracy of the four filters decreases with the increase of λ_c, however, the NNIWGG-J-GLMB filter always has the best tracking accuracy compared with the other three filters.

Fig. 5a and Fig. 5b respectively give the average OSPA and OSPA$^{(2)}$ distances at the probability of detection levels 0.60, 0.70, 0.80, 0.90, 0.95 and 0.98 with $P_g = 0.10$, $\lambda_c = 10$,

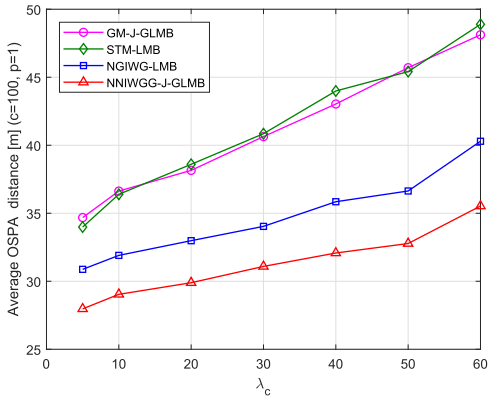

(a) Average OSPA distances

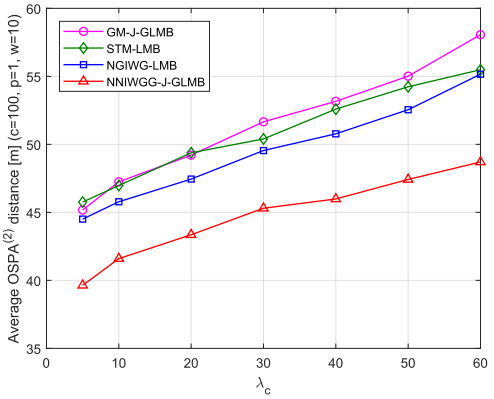

(b) Average OSPA$^{(2)}$ distances

FIGURE 4. Average OSPA and OSPA$^{(2)}$ distances of the four filters with different λ_c.

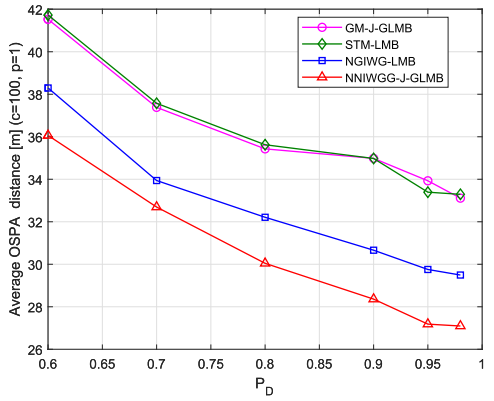

(a) Average OSPA distances

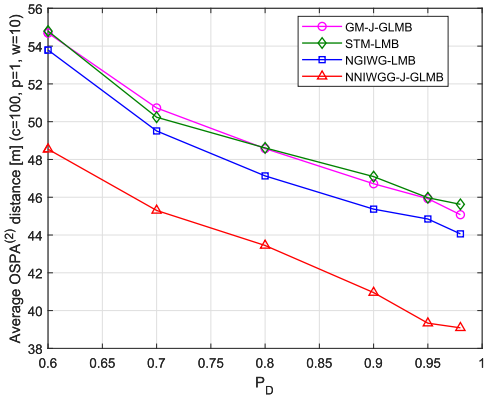

(b) Average OSPA$^{(2)}$ distances

FIGURE 5. Average OSPA and OSPA$^{(2)}$ distances of the four filters with different P_D.

$\rho = 0.90$, $N_{\max} = 5$. As can be seen from the figures, the performance of the four filters is significantly improved with the increase of P_D. These findings suggest that the proposed filter can still show good performance even at low detection probability.

Fig. 6a and Fig. 6b respectively display the average OSPA and OSPA$^{(2)}$ distances for $P_g = 0$, 0.02, 0.10, 0.20, 0.30, 0.40 when $P_D = 0.95$, $\lambda_c = 10$, $\rho = 0.90$, $N_{\max} = 5$. It can be seen that the performance of the four filters decreases with the increase of P_g, however, the proposed filter still has the smallest OSPA and OSPA$^{(2)}$ distances. When $P_g = 0$, that is, there is no non-stationary HTMN, the GM-J-GLMB filter, STM-LMB filter and NGIWG-LMB filter have comparable OSPA and OSPA$^{(2)}$ distances. This is mainly because when there is no non-stationary HTMN, the measurement noise as shown in (82) follows a Gaussian distribution with unknown mean. Moreover, the NGIWG-LMB filter and STM-LMB filter will reduce to the GM-LMB filter. Since the proposed filter has unknown mean Student's t-distribution measurement noise model, while the other three filters formulate the measurement noise as zero-mean Gaussian distribution and Student's t-distribution respectively. It is worth noting that the OSPA distance and OSPA$^{(2)}$ distance differences between the four filters are prone to increase with the increase of P_g, which suggests that the proposed filter is robust to non-stationary HTMN.

To sum up, the tracking accuracy of the STM-LMB filter is similar to that of the GM-J-GLMB filter. Although the process and measurement noises of the STM-LMB filter are modeled as Student's t distribution to handle the heavy-tailed noises [33], the non-stationary heavy-tailed noise is considered in this paper. In this case, the STM-LMB filter still can not achieve ideal tracking accuracy.

To illustrate the influence of $N_{\max}$ and ρ on the performance of the proposed filter, the average OSPA and OSPA$^{(2)}$ distances under different $N_{\max}$ and ρ are compared when other parameters are fixed.

Fig. 7 gives the average OSPA and OSPA$^{(2)}$ distances of the proposed filter with different $N_{\max}$. It can be seen that the proposed filter can achieve relatively small average OSPA and OSPA$^{(2)}$ distances after $N_{\max} = 3$ iterations, and it has the best performance when $N_{\max} = 5$. In conclusion, the results show that $N_{\max}$ will affect the performance of the proposed filter, but this effect can be almost ignored when $N_{\max} \geq 3$.

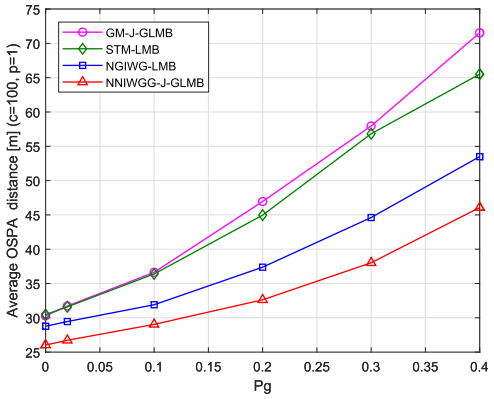

(a) Average OSPA distances

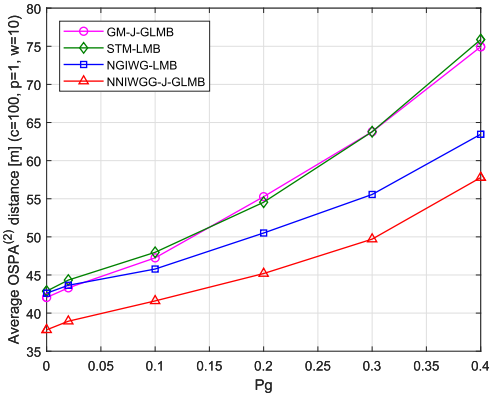

(b) Average OSPA$^{(2)}$ distances

FIGURE 6. Average OSPA and OSPA$^{(2)}$ distances of the four filters with different P_g.

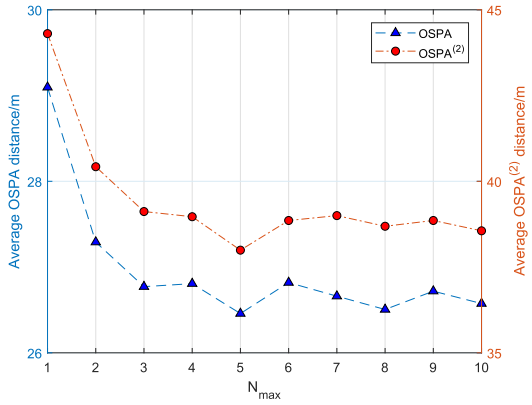

FIGURE 7. Average OSPA and OSPA$^{(2)}$ distances of the NNIWGG-J-GLMB filter with different $N_{\max}$.

Fig. 8 provides the average OSPA and OSPA$^{(2)}$ distances of the proposed filter with different ρ over 100 MC trials. It is suggested that the OSPA and OSPA$^{(2)}$ distances are not very sensitive to ρ when it is greater than 0.85, and a good performance can be achieved when $\rho \in [0.85, 1]$.

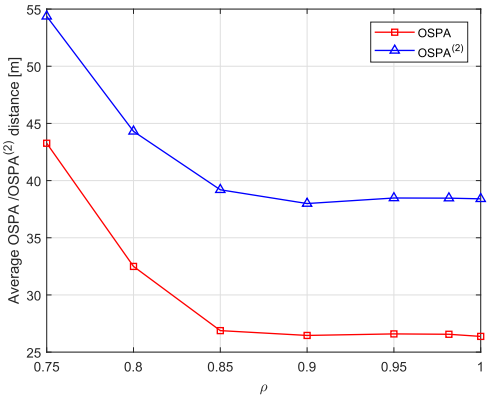

FIGURE 8. Average OSPA and OSPA$^{(2)}$ distances of the NNIWGG-J-GLMB filter with different ρ.

B. NONLINEAR SCENARIOS

To further evaluate the performance of the NNIWGG-J-GLMB filter in nonlinear scenarios with unknown non-stationary HTMN, the Taylor series approximations of nonlinear state function $f(\cdot)$ and measurement function $h(\cdot)$ can be obtained by extended Kalman filter (EKF).

The nonlinear scenarios are employed as in [32]. The bearing-range sensor is placed at (0, 0), and it is assumed that the sensor receives measurements containing non-stationary HTMN, namely $\boldsymbol{z}_k = [\theta_k, r_k]^{\mathrm{T}}$, and the sensor has the following function

$$\boldsymbol{z}_k = \begin{bmatrix} \arctan\frac{p_{y,k}}{p_{x,k}} \\ \sqrt{p_{x,k}^2 + p_{y,k}^2} \end{bmatrix} + \boldsymbol{\varepsilon}_k \tag{85}$$

The non-stationary HTMN $\boldsymbol{\varepsilon}_k$ can be obtained by

$$\boldsymbol{\varepsilon}_k \sim \begin{cases} \mathrm{N}(\boldsymbol{\mu}_k, \boldsymbol{R}_k) & \text{with probability } 1 - P_g \\ \mathrm{N}(\boldsymbol{\mu}_k, 25\boldsymbol{R}_k) & \text{with probability } P_g \end{cases} \tag{86}$$

where $\boldsymbol{R}_k = \mathrm{diag}([2(\pi/180), 10])^2$ is the nominal measurement noise variance matrix. Moreover, the true mean vector of measurement noise can be represented by

$$\boldsymbol{\mu}_k = \begin{cases} [(\pi/180)\ \text{rad};\ 5\ \text{m}], & k \in (0, 30\ \text{s}] \\ [2(\pi/180)\ \text{rad};\ 10\ \text{m}], & k \in (30\ \text{s}, 60\ \text{s}] \\ [(\pi/180)\ \text{rad};\ 5\ \text{m}], & k \in (60\ \text{s}, 100\ \text{s}] \end{cases} \tag{87}$$

The birth target model is an LMB RFS with parameters $\pi_B = \{r_B^{(i)}, p_B^{(i)}(\zeta)\}_{i=1}^4$, where $r_B^{(i)} = 0.03$, and the single target PDF is modeled as the NNIWGG model as shown in (84) with $\boldsymbol{m}_B^{(1)} = [-1500, 0, 250, 0, 0]^{\mathrm{T}}$, $\boldsymbol{m}_B^{(2)} = [-250, 0, 1000, 0, 0]^{\mathrm{T}}$, $\boldsymbol{m}_B^{(3)} = [250, 0, 750, 0, 0]^{\mathrm{T}}$, $\boldsymbol{m}_B^{(4)} = [1000, 0, 1500, 0, 0]^{\mathrm{T}}$, $\boldsymbol{P}_B = \mathrm{diag6}([50, 50, 50, 50, (\pi/180)]^{\mathrm{T}})^2$, $\boldsymbol{\eta}_B = [0; 0]$, $\beta_B = 1$, $t_B = 5$, $\boldsymbol{T}_B = \mathrm{diag}([5, \pi/180]^{\mathrm{T}})^2$, $a_B = 5$, $b_B = 1$. The remaining parameters are the same as that in Section IV-A.

Fig. 9 gives the true trajectories, measurements and estimated trajectories of a single trial obtained by the four filters with $P_g = 0.10$, $P_D = 0.95$, $\lambda_c = 20$, $\rho = 0.90$, and

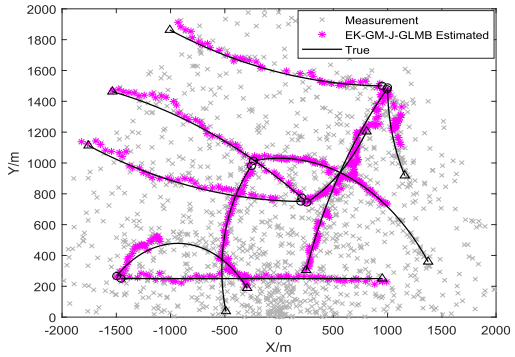

(a) EK-GM-J-GLMB filter

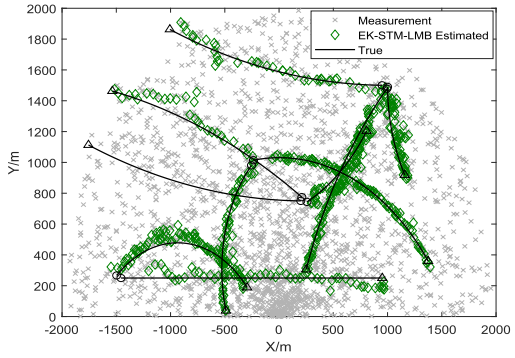

(b) EK-STM-LMB filter

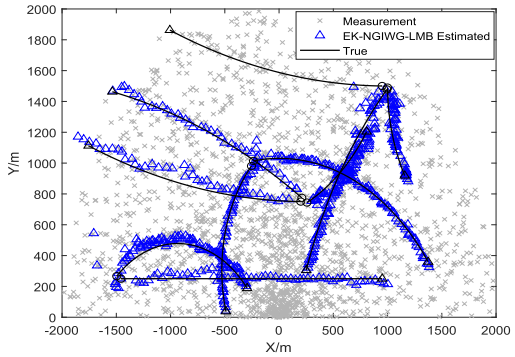

(c) EK-NGIWG-LMB filter

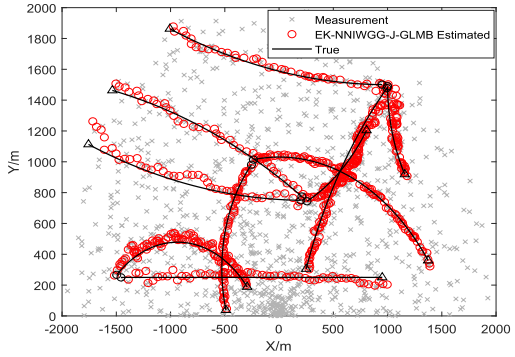

(d) EK-NNIWGG-J-GLMB filter

FIGURE 9. The ground truth (black lines) and estimated trajectories (colored labels) of the four filters.

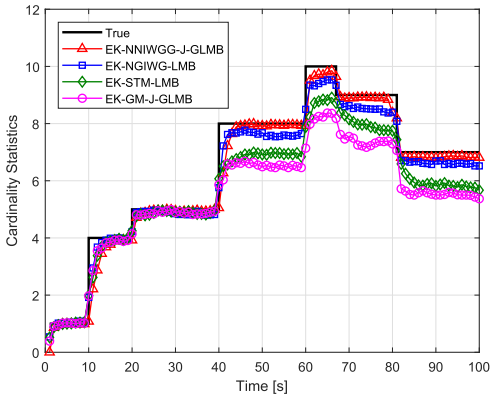

FIGURE 10. The true and estimated cardinality for the four filters over time.

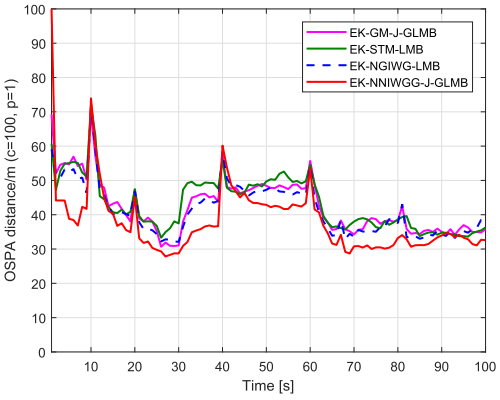

(a) OSPA distances

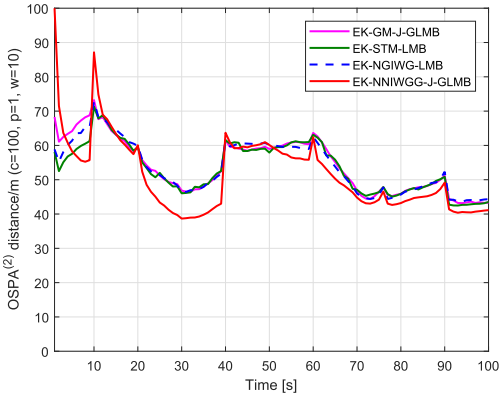

(b) OSPA$^{(2)}$ distances

FIGURE 11. OSPA and OSPA$^{(2)}$ distances for the four filters over time.

$N_{\max} = 5$. The EK-GM-J-GLMB filter, EK-STM-LMB filter and EK-NGIWG-LMB filter all have target trajectories loss in the tracking period, while the proposed filter can estimate all target trajectories correctly, as is shown in Fig.9.

It can be seen from Fig.10 that the change of the mean of non-stationary HTMN makes it impossible for the three existing filters to get correct cardinality estimations,

especially after 40 s, there is an obvious underestimation with the increase of the number of targets and the continuous change of HTMN mean. By contrast, the cardinality estimation of the proposed EK-NNIWGG-J-GLMB filter is better than that of the above three filters.

Fig.11a and Fig.11b respectively show the comparison of the average OSPA and OSPA$^{(2)}$ distances of the four filters. It can be seen that the proposed filter has the smallest average OSPA and OSPA$^{(2)}$ distances, that is, the proposed filter has the best tracking accuracy among the four filters.

V. CONCLUSION

A robust J-GLMB filter referred to as the NNIWGG-J-GLMB filter is proposed for MTT under non-stationary HTMN in this paper. To handle unknown non-stationary HTMN, we develop the measurement model using the Student's t-distribution with unknown and time-varying mean. The mean vector and scale matrix of measurement noise are modeled as a Normal-IW distribution, while the DOF and the auxiliary variable are modeled as Gamma distributions. Hence, the target state is augmented by the noise parameters and kinematic state, and the NNIWGG-J-GLMB filter is derived by applying the VB approach. The proposed filter is implemented by expressing the joint posterior multitarget density as mixtures of the Gaussian, Normal-IW, and Gamma distributions. The proposed filter is investigated by MTT scenarios with unknown non-stationary HTMN. Simulation results suggest that the proposed NNIWGG-J-GLMB filter can perform an improved performance than that of the GM-J-GLMB filter, STM-LMB filter and NGIWG-LMB filter for unknown non-stationary HTMN in both linear and nonlinear scenarios.

APPENDICES

APPENDIX A
PROOF OF LEMMA 2

Proof: Assume that the variables in $\boldsymbol{\zeta}$ are mutually independent. Exploiting (20), the joint posterior PDF can be written as

$$\begin{aligned} p(\boldsymbol{\zeta}|z_{1:k}) &\propto p(z_k|\boldsymbol{\zeta})p(\boldsymbol{\zeta}|z_{1:k-1}) \\ &= p(z_k|\boldsymbol{x},\boldsymbol{\mu},\boldsymbol{R},\lambda)p(\boldsymbol{x}|z_{1:k-1}) \\ &\quad \times p(\boldsymbol{\mu},\boldsymbol{R}|z_{1:k-1})p(\lambda|v)p(v|z_{1:k-1}) \end{aligned} \tag{88}$$

Substituting (6)-(8), and (14)-(15) into (88) yields

$$\begin{aligned} &p(z_k,\boldsymbol{\zeta}|z_{1:k-1}) \\ &\quad \propto \mathrm{N}(z_k;\boldsymbol{H}\boldsymbol{x}+\boldsymbol{\mu},\boldsymbol{R}/\lambda)\mathrm{N}(\boldsymbol{x}|\boldsymbol{m}_{k|k-1},\boldsymbol{P}_{k|k-1}) \\ &\qquad \times \mathrm{N}(\boldsymbol{\mu};\boldsymbol{\eta}_{k|k-1},\beta_{k|k-1}\boldsymbol{R})\mathrm{IW}(\boldsymbol{R};t_{k|k-1},\boldsymbol{T}_{k|k-1}) \\ &\qquad \times \mathrm{G}(\lambda;v/2,v/2)\mathrm{G}(v;a_{k|k-1},b_{k|k-1})p(z_{1:k-1}) \end{aligned} \tag{89}$$

Unfortunately, since the state $\boldsymbol{x}$, unknown parameters $\boldsymbol{\mu}$, $\boldsymbol{R}$ and v, and λ are coupled, it is challenging to get an available analytical solution for the joint posterior PDF.

By means of the VB approach, the log marginal likelihood $\ln p(z_k|z_{1:k-1})$ can be expressed as

$$\begin{aligned} \ln p(z_k|z_{1:k-1}) &= \mathrm{L}(q(\boldsymbol{x})q(\boldsymbol{\mu})q(\boldsymbol{R})q(\lambda)q(v)) \\ &\quad +\mathrm{KL}(q(\boldsymbol{x})q(\boldsymbol{\mu})q(\boldsymbol{R})q(\lambda)q(v) \parallel p(\boldsymbol{\zeta}|z_{1:k})) \end{aligned} \tag{90}$$

where $\mathrm{KL}(\cdot)$ represents the Kullback-Leibler divergence between the true posterior PDF $p(\boldsymbol{\zeta}|z_{1:k})$ and the approximated PDF $q(\boldsymbol{x})q(\boldsymbol{\mu})q(\boldsymbol{R})q(\lambda)q(v)$, namely,

$$\begin{aligned} &\mathrm{KL}(q(\boldsymbol{x})q(\boldsymbol{\mu})q(\boldsymbol{R})q(\lambda)q(v) \parallel p(\boldsymbol{\zeta}|z_{1:k})) \\ &= \int q(\boldsymbol{x})q(\boldsymbol{\mu})q(\boldsymbol{R})q(\lambda)q(v)\ln\left(\frac{q(\boldsymbol{x})q(\boldsymbol{\mu})q(\boldsymbol{R})q(\lambda)q(v)}{p(\boldsymbol{\zeta}|z_{1:k})}\right)d\boldsymbol{\zeta} \end{aligned} \tag{91}$$

and $\mathrm{L}(q(\boldsymbol{x})q(\boldsymbol{\mu})q(\boldsymbol{R})q(\lambda)q(v))$ is the variational lower bound of $\ln p(z_k|z_{1:k-1})$ specified as

$$\begin{aligned} &\mathrm{L}(q(\boldsymbol{x})q(\boldsymbol{\mu})q(\boldsymbol{R})q(\lambda)q(v)) \\ &= \int q(\boldsymbol{x})q(\boldsymbol{\mu})q(\boldsymbol{R})q(\lambda)q(v)\ln\left(\frac{p(z_k,\boldsymbol{\zeta}|z_{1:k-1})}{q(\boldsymbol{x})q(\boldsymbol{\mu})q(\boldsymbol{R})q(\lambda)q(v)}\right)d\boldsymbol{\zeta} \end{aligned} \tag{92}$$

According to (91), the approximated PDF can be obtained by minimizing the KL divergence which is always non-negative. As shown in (90), minimizing the KL divergence is equivalent to obtaining the lower bound of $\ln p(z_k|z_{1:k-1})$. Therefore, a fixed-point iteration is used to achieve the approximations of $q(\boldsymbol{x})$, $q(\boldsymbol{\mu},\boldsymbol{R})$, $q(\lambda)$ and $q(v)$ by iteratively solving the following equations,

$$\ln q(\boldsymbol{x}) = \mathrm{E}_{\boldsymbol{\mu},\boldsymbol{R},\lambda,v}[\ln p(z_k,\boldsymbol{\zeta}|z_{1:k-1})] + C_{\boldsymbol{x}} \tag{93}$$

$$\ln q(\boldsymbol{\mu},\boldsymbol{R}) = \mathrm{E}_{\boldsymbol{x},\lambda,v}[\ln p(z_k,\boldsymbol{\zeta}|z_{1:k-1})] + C_{\boldsymbol{\mu},\boldsymbol{R}} \tag{94}$$

$$\ln q(\lambda) = \mathrm{E}_{\boldsymbol{x},\boldsymbol{\mu},\boldsymbol{R},v}[\ln p(z_k,\boldsymbol{\zeta}|z_{1:k-1})] + C_{\lambda} \tag{95}$$

$$\ln q(v) = \mathrm{E}_{\boldsymbol{x},\boldsymbol{\mu},\boldsymbol{R},\lambda}[\ln p(z_k,\boldsymbol{\zeta}|z_{1:k-1})] + C_{v} \tag{96}$$

where $\mathrm{E}_{\varpi}[\cdot]$ denotes the expectation operation with respect to ϖ, and $C_{\boldsymbol{x}}$, $C_{\boldsymbol{\mu},\boldsymbol{R}}$, C_{λ} and C_{v} are the constants independent of the state $\boldsymbol{x}$, the mean vector $\boldsymbol{\mu}$ and the scale matrix $\boldsymbol{R}$, the auxiliary variable λ, and the DOF v, respectively.

Substituting (89) into (93), we have

$$\begin{aligned} &\ln q(\boldsymbol{x}) \\ &= \ln \mathrm{N}(\boldsymbol{x};\boldsymbol{m}_{k|k-1},\boldsymbol{P}_{k|k-1}) \\ &\quad -\frac{1}{2}(z_k-\boldsymbol{H}\boldsymbol{x}-\mathrm{E}[\boldsymbol{\mu}])^{\mathrm{T}}\mathrm{E}[\lambda]\mathrm{E}[\boldsymbol{R}^{-1}](z_k-\boldsymbol{H}\boldsymbol{x}-\mathrm{E}[\boldsymbol{\mu}]) \\ &\quad +C_{\boldsymbol{x}} \end{aligned} \tag{97}$$

Define the modified scale matrix $\tilde{\boldsymbol{R}}_k$ as

$$\tilde{\boldsymbol{R}}_k = \{\mathrm{E}[\boldsymbol{R}^{-1}]\}^{-1}/\mathrm{E}[\lambda] \tag{98}$$

Substituting (98) into (97) yields

$$\begin{aligned} \ln q(\boldsymbol{x}) &= \ln \mathrm{N}(\boldsymbol{x};\boldsymbol{m}_{k|k-1},\boldsymbol{P}_{k|k-1}) \\ &\quad +\ln \mathrm{N}(z_k;\boldsymbol{H}x+\mathrm{E}[\boldsymbol{\mu}],\tilde{\boldsymbol{R}}_k)+C_{\boldsymbol{x}} \end{aligned} \tag{99}$$

Exploiting (99), the posterior PDF $q(\boldsymbol{x})$ is given by

$$q(\boldsymbol{x}) \propto \mathrm{N}(\boldsymbol{x};\boldsymbol{m}_{k|k-1},\boldsymbol{P}_{k|k-1})\mathrm{N}(z_k;\boldsymbol{H}\boldsymbol{x}+\mathrm{E}[\boldsymbol{\mu}],\tilde{\boldsymbol{R}}_k) \tag{100}$$

According to (100) and the Bayes's rule, and using the measurement update of the Kalman filter, we can obtain (25), (29)-(32).

Substituting (89) into (94) gives

$$\begin{aligned}\ln q(\boldsymbol{\mu},\boldsymbol{R}) = &\ln \mathrm{N}(\boldsymbol{\mu};\boldsymbol{\eta}_{k|k-1},\beta_{k|k-1}\boldsymbol{R})\\ &+\ln \mathrm{N}(\boldsymbol{\mu};z_k-\boldsymbol{H}\boldsymbol{m}_k,\boldsymbol{R}/\mathrm{E}[\lambda])\\ &-\frac{1}{2}\mathrm{E}[\lambda]\mathrm{tr}\left(\boldsymbol{H}\boldsymbol{P}_k\boldsymbol{H}^{\mathrm{T}}\boldsymbol{R}^{-1}\right)-\frac{1}{2}\mathrm{tr}\left(\boldsymbol{T}_{k|k-1}\boldsymbol{R}^{-1}\right)\\ &-\frac{m+t_{k|k-1}+1}{2}\ln|\boldsymbol{R}|+C_{\boldsymbol{\mu},\boldsymbol{R}}\end{aligned}\tag{101}$$

The approximated density of $\boldsymbol{\mu}$ conditioned on $\boldsymbol{R}$ is given by [39]

$$\begin{aligned}\ln q(\boldsymbol{\mu}) = &\ln \mathrm{N}(\boldsymbol{\mu};\boldsymbol{\eta}_{k|k-1},\beta_{k|k-1}\boldsymbol{R})\\ &+\ln \mathrm{N}(\boldsymbol{\mu};z_k-\boldsymbol{H}\boldsymbol{m}_k,\boldsymbol{R}/\mathrm{E}[\lambda])+C_{\boldsymbol{\mu}}\end{aligned}\tag{102}$$

Let $\tilde{z}_k = z_k - \boldsymbol{H}\boldsymbol{m}_k$, and exploiting the Gaussian identities, $q(\boldsymbol{\mu})$ is given as

$$q(\boldsymbol{\mu}) = \mathrm{N}(\boldsymbol{\mu};\boldsymbol{\eta}_k,\beta_k\boldsymbol{R})+C_{\boldsymbol{\mu}}\tag{103}$$

where $\boldsymbol{\eta}_k$ and β_k are given by (33)-(36).

Then we consider the approximated density of $\boldsymbol{R}$ via calculating the expectation with respect to $\boldsymbol{R}$ and subtracting (102) yields

$$\begin{aligned}\ln q(\boldsymbol{R}) = &-\frac{m+t_{k|k-1}+1+1}{2}\ln|\boldsymbol{R}|\\ &-\frac{1}{2}\mathrm{tr}\left\{\left(\boldsymbol{T}_{k|k-1}+\mathrm{E}[\lambda]\boldsymbol{A}_k\right)\boldsymbol{R}^{-1}\right\}+C_{\boldsymbol{R}}\end{aligned}\tag{104}$$

where $\boldsymbol{A}_k$ is given in (39). According to (104), $q(\boldsymbol{R})$ is formulated as

$$q(\boldsymbol{R}) = \mathrm{IW}(\boldsymbol{R};t_k,\boldsymbol{T}_k)\tag{105}$$

where t_k and $\boldsymbol{T}_k$ are given by (37) and (38), respectively.

Substituting (89) into (95), we get

$$\begin{aligned}\ln q(\lambda) = &\left(\frac{\mathrm{E}[v]+m}{2}-1\right)\ln\lambda\\ &-\frac{1}{2}\lambda\left(\mathrm{E}[v]+\mathrm{tr}\left\{\boldsymbol{B}_k\mathrm{E}[\boldsymbol{R}^{-1}]\right\}\right)+C_{\lambda}\end{aligned}\tag{106}$$

where $\boldsymbol{B}_k$ is given in (42). According to (106), (40)-(41) and (52)-(53) can be obtained. In addition, $q(\lambda)$ is formulated as (27).

Substituting (89) into (96), we obtain

$$\begin{aligned}\ln q(v) = &\frac{v}{2}\ln\frac{v}{2}-\ln\Gamma\left(\frac{v}{2}\right)+\left(\frac{v}{2}-1\right)\mathrm{E}[\ln\lambda]\\ &-\frac{v}{2}\mathrm{E}[\lambda]+(a_{k|k-1}-1)\ln v-b_{k|k-1}v+C_v\end{aligned}\tag{107}$$

Using Stirling's approximation: $\ln\Gamma(v/2)\approx[(v-1)/2]\ln(v/2)-(v/2)$, $\ln q(v)$ can be rewritten as

$$\begin{aligned}\ln q(v) = &\left(a_{k|k-1}+\frac{1}{2}-1\right)\ln v\\ &-\left(b_{k|k-1}-\frac{1}{2}-\frac{1}{2}\mathrm{E}[\ln\lambda]+\frac{1}{2}\mathrm{E}[\lambda]\right)v+C_v\end{aligned}\tag{108}$$

According to (108), (28) and (46)-(47) can be obtained.

APPENDIX B
DERIVATION OF (56)

Proof: According to (90)-(92), the marginal likelihood $p(\boldsymbol{z}_k|\boldsymbol{z}_{1:k-1})$ can be obtained approximately from

$$p(\boldsymbol{z}_k|\boldsymbol{z}_{1:k-1})\approx q(\boldsymbol{z}_k)=\exp\left(\mathrm{L}(q(\boldsymbol{x})q(\boldsymbol{\mu})q(\boldsymbol{R})q(\lambda)q(v))\right)\tag{109}$$

For simplicity, $\mathrm{L}(q(\boldsymbol{x})q(\boldsymbol{\mu})q(\boldsymbol{R})q(\lambda)q(v))$ is represented by L in the following derivation. And then, L can be formulated as

$$\mathrm{L}=\mathrm{E}\left[\ln p(\boldsymbol{z}_k,\boldsymbol{\zeta}|\boldsymbol{z}_{1:k-1})\right]-\mathrm{E}\left[\ln\left(q(\boldsymbol{x})q(\boldsymbol{\mu})q(\boldsymbol{R})q(\lambda)q(v)\right)\right]\tag{110}$$

where $\mathrm{E}[\cdot]$ indicates $\mathrm{E}_{\boldsymbol{x},\boldsymbol{\mu},\boldsymbol{R},\lambda,v}[\cdot]$. In addition, let $\mathrm{L}_1 \triangleq \mathrm{E}\left[\ln p(\boldsymbol{z}_k,\boldsymbol{\zeta}|\boldsymbol{z}_{1:k-1})\right]$, and $\mathrm{L}_2 \triangleq \mathrm{E}\left[\ln\left(q(x)q(\mu)q(R)q(\lambda)q(v)\right)\right]$, respectively.

Substituting (89) into the first part on the right of (110) gives

$$\begin{aligned}\mathrm{L}_1 = &\mathrm{E}[\ln\mathrm{N}(\boldsymbol{z}_k;\boldsymbol{H}\boldsymbol{x}+\boldsymbol{\mu},\boldsymbol{R}/\lambda)]\\ &+\mathrm{E}[\ln\mathrm{N}(\boldsymbol{x};\boldsymbol{m}_{k|k-1},\boldsymbol{P}_{k|k-1})]\\ &+\mathrm{E}[\ln\mathrm{N}(\boldsymbol{\mu};\boldsymbol{\eta}_{k|k-1},\beta_{k|k-1}\boldsymbol{R})]\\ &+\mathrm{E}[\ln\mathrm{IW}(\boldsymbol{R};t_{k|k-1},\boldsymbol{T}_{k|k-1})]\\ &+\mathrm{E}[\ln\mathrm{G}(\lambda;v/2,v/2)]\\ &+\mathrm{E}[\ln\mathrm{G}(v;a_{k|k-1},b_{k|k-1})]\end{aligned}\tag{111}$$

where

$$\begin{aligned}&\mathrm{E}[\ln\mathrm{N}(\boldsymbol{z}_k;\boldsymbol{H}\boldsymbol{x}+\boldsymbol{\mu},\boldsymbol{R}/\lambda)]\\ &=-\frac{m}{2}\ln(2\pi)-\frac{1}{2}\mathrm{E}[\ln|\boldsymbol{R}|]\\ &\quad+\frac{m}{2}\mathrm{E}[\ln\lambda]-\frac{1}{2}\mathrm{tr}\left(\mathrm{E}[\lambda]\mathrm{E}[\boldsymbol{R}^{-1}](\tilde{\boldsymbol{z}}_k-\boldsymbol{\eta}_k)(\tilde{\boldsymbol{z}}_k-\boldsymbol{\eta}_k)^{\mathrm{T}}\right)\\ &\quad-\frac{1}{2}\mathrm{tr}\left(\mathrm{E}[\lambda]\mathrm{E}[\boldsymbol{R}^{-1}]\left(\boldsymbol{H}\boldsymbol{P}_k\boldsymbol{H}^{\mathrm{T}}+\boldsymbol{P}_{\boldsymbol{\mu}}\right)\right)\end{aligned}\tag{112}$$

$$\begin{aligned}&\tilde{\boldsymbol{z}}_k\\ &=\boldsymbol{z}_k-\boldsymbol{H}\boldsymbol{m}_k\end{aligned}\tag{113}$$

$$\begin{aligned}&\mathrm{E}[\ln\mathrm{N}(\boldsymbol{x};\boldsymbol{m}_{k|k-1},\boldsymbol{P}_{k|k-1})]\\ &=-\frac{n}{2}\ln(2\pi)-\frac{1}{2}\ln|\boldsymbol{P}_{k|k-1}|\\ &\quad-\frac{1}{2}\mathrm{tr}\left(\boldsymbol{P}_{k|k-1}^{-1}\mathrm{E}[(\boldsymbol{x}-\boldsymbol{m}_{k|k-1})(\boldsymbol{x}-\boldsymbol{m}_{k|k-1})^{\mathrm{T}}]\right)\\ &=-\frac{n}{2}\ln(2\pi)-\frac{1}{2}\ln|\boldsymbol{P}_{k|k-1}|\\ &\quad-\frac{1}{2}\mathrm{tr}\left(\boldsymbol{P}_{k|k-1}^{-1}\left[\boldsymbol{P}_k+(\boldsymbol{m}_k-\boldsymbol{m}_{k|k-1})(\boldsymbol{m}_k-\boldsymbol{m}_{k|k-1})^{\mathrm{T}}\right]\right)\end{aligned}\tag{114}$$

$$\begin{aligned}&\mathrm{E}[\ln\mathrm{N}(\boldsymbol{\mu};\boldsymbol{\eta}_{k|k-1},\beta_{k|k-1}\boldsymbol{R})]\\ &=-\frac{m}{2}\ln(2\pi)-\frac{1}{2}\mathrm{E}[\ln|\boldsymbol{R}|]-\frac{m}{2}\ln\beta_{k|k-1}\\ &\quad-\frac{1}{2}\mathrm{tr}\left(\frac{\mathrm{E}[\boldsymbol{R}^{-1}]}{\beta_{k|k-1}}[\boldsymbol{P}_{\boldsymbol{\mu}}+(\boldsymbol{\eta}_k-\boldsymbol{\eta}_{k|k-1})(\boldsymbol{\eta}_k-\boldsymbol{\eta}_{k|k-1})^{\mathrm{T}}]\right)\end{aligned}\tag{115}$$

$$\begin{aligned}&\mathrm{E}[\ln \mathrm{IW}(\boldsymbol{R};\, t_{k|k-1}, \boldsymbol{T}_{k|k-1})]\\&= \frac{t_{k|k-1}}{2}\ln|\boldsymbol{T}_{k|k-1}| - \frac{m}{2}t_{k|k-1}\ln 2 - \ln\Gamma\left(\frac{t_{k|k-1}}{2}\right)\\&\quad -\frac{m+t_{k|k-1}+1}{2}\mathrm{E}[\ln|\boldsymbol{R}|] - \frac{1}{2}\mathrm{tr}\left(\mathrm{E}[\boldsymbol{R}^{-1}]\boldsymbol{T}_{k|k-1}\right) \quad (116)\\&\mathrm{E}[\ln \mathrm{G}(\lambda;\, v/2, v/2)]\\&= \frac{1}{2}\mathrm{E}\left[\ln\frac{v}{2}\right] + \frac{1}{2}\mathrm{E}[v]\\&\quad +\left(\frac{1}{2}\mathrm{E}[v]-1\right)\mathrm{E}[\ln\lambda] - \frac{1}{2}\mathrm{E}[v]\,\mathrm{E}[\lambda] \quad (117)\\&\mathrm{E}[\ln \mathrm{G}(v;\, a_{k|k-1}, b_{k|k-1})]\\&= a_{k|k-1}\ln b_{k|k-1}\\&\quad -\ln\Gamma(a_{k|k-1}) + (a_{k|k-1}-1)\mathrm{E}[\ln v] - b_{k|k-1}\mathrm{E}[v] \quad (118)\end{aligned}$$

The second term on the right of (110) can be calculated by

$$\begin{aligned}\mathrm{L}_2 = {}&\mathrm{E}[\ln \mathrm{N}(\boldsymbol{x};\, \boldsymbol{m}_k, \boldsymbol{P}_k)] + \mathrm{E}[\ln \mathrm{N}(\boldsymbol{\mu};\, \boldsymbol{\eta}_k, \beta_k\boldsymbol{R})]\\&+\mathrm{E}[\ln \mathrm{IW}(\boldsymbol{R};\, t_k, \boldsymbol{T}_k)] + \mathrm{E}[\ln \mathrm{G}(\lambda;\, c_k, d_k)]\\&+\mathrm{E}[\ln \mathrm{G}(v;\, a_k, b_k)] \quad (119)\end{aligned}$$

where

$$\begin{aligned}&\mathrm{E}[\ln \mathrm{N}(\boldsymbol{x};\, \boldsymbol{m}_k, \boldsymbol{P}_k)]\\&= -\frac{n}{2}\ln(2\pi) - \frac{1}{2}\ln|\boldsymbol{P}_k|\\&\quad -\frac{1}{2}\mathrm{tr}\left(\boldsymbol{P}_k^{-1}\mathrm{E}[(\boldsymbol{x}-\boldsymbol{m}_k)(\boldsymbol{x}-\boldsymbol{m}_k)^{\mathrm{T}}]\right)\\&= -\frac{n}{2}\ln(2\pi) - \frac{1}{2}\ln|\boldsymbol{P}_k| - \frac{n}{2} \quad (120)\\&\mathrm{E}[\ln \mathrm{N}(\boldsymbol{\mu};\, \boldsymbol{\eta}_k, \beta_k\boldsymbol{R})]\\&= -\frac{m}{2}\ln 2\pi - \frac{1}{2}\mathrm{E}[\ln|\boldsymbol{R}|]\\&\quad -\frac{m}{2}\ln\beta_k - \frac{1}{2}\mathrm{tr}\left(\frac{\mathrm{E}[\boldsymbol{R}^{-1}]}{\beta_k}\mathrm{E}[(\boldsymbol{\mu}-\boldsymbol{\eta}_k)(\boldsymbol{\mu}-\boldsymbol{\eta}_k)^{\mathrm{T}}]\right)\\&= -\frac{m}{2}\ln(2\pi) - \frac{1}{2}\mathrm{E}[\ln|\boldsymbol{R}|] - \frac{m}{2}\ln\beta_k - \frac{m}{2} \quad (121)\\&\mathrm{E}[\ln \mathrm{IW}(\boldsymbol{R};\, t_k, \boldsymbol{T}_k)]\\&= \frac{t_k}{2}\ln|\boldsymbol{T}_k| - \frac{m}{2}t_k\ln 2\\&\quad -\ln\Gamma\left(\frac{t_k}{2}\right) - \frac{m+t_k+1}{2}\mathrm{E}[\ln|\boldsymbol{R}|] - \frac{1}{2}\mathrm{tr}\left(\mathrm{E}[\boldsymbol{R}^{-1}]\boldsymbol{T}_k\right)\\&\quad (122)\\&\mathrm{E}[\ln \mathrm{G}(\lambda;\, c_k, d_k)]\\&= c_k\ln d_k - \ln\Gamma(c_k) + (c_k-1)\mathrm{E}[\ln\lambda] - d_k\mathrm{E}[\lambda] \quad (123)\\&\mathrm{E}[\ln \mathrm{G}(v;\, a_k, b_k)]\\&= a_k\ln b_k - \ln\Gamma(a_k) + (a_k-1)\mathrm{E}[\ln v] - b_k\mathrm{E}[v] \quad (124)\end{aligned}$$

Substituting (111) and (119) into (110), and exploiting (97)-(108), the likelihood function $q(\mathbf{z}_k)$ can be approximately calculated as (56).

REFERENCES

[1] T. Fortmann, Y. Bar-Shalom, and M. Scheffe, "Sonar tracking of multiple targets using joint probabilistic data association," *IEEE J. Ocean. Eng.*, vol. OE-8, no. 3, pp. 173–184, Jul. 1983.
[2] Y. Bar-Shalom, X. Li, and T. Kirubarajan, *Estimation With Applications to Tracking and Navigation*. New York, NY, USA: Wiley, 2001.
[3] S. S. Blackman, "Multiple hypothesis tracking for multiple target tracking," *IEEE Aerosp. Electron. Syst. Mag.*, vol. 19, no. 1, pp. 5–18, Jan. 2004.
[4] R. S. Mahler, *Statistical Multisource-Multitarget Information Fusion*. Norwood, MA, USA: Artech House, 2007.
[5] R. S. Mahler, *Advances in Statistical Multisource-Multitarget Information Fusion*. Norwood, MA, USA: Artech House, 2014.
[6] R. P. S. Mahler, "Multitarget Bayes filtering via first-order multitarget moments," *IEEE Trans. Aerosp. Electron. Syst.*, vol. 39, no. 4, pp. 1152–1178, Oct. 2003.
[7] R. Mahler, "PHD filters of higher order in target number," *IEEE Trans. Aerosp. Electron. Syst.*, vol. 43, no. 99, pp. 1523–1543, Oct. 2007.
[8] B.-T. Vo, B.-N. Vo, and A. Cantoni, "The cardinality balanced multi-target multi-Bernoulli filter and its implementations," *IEEE Trans. Signal Process.*, vol. 57, no. 2, pp. 409–423, Feb. 2009.
[9] B.-T. Vo and B.-N. Vo, "Labeled random finite sets and multi-object conjugate priors," *IEEE Trans. Signal Process.*, vol. 61, no. 13, pp. 3460–3475, Jul. 2013.
[10] B.-N. Vo, B.-T. Vo, and D. Phung, "Labeled random finite sets and the Bayes multi-target tracking filter," *IEEE Trans. Signal Process.*, vol. 62, no. 24, pp. 6554–6567, Dec. 2014.
[11] S. Reuter, B. T. Vo, B. N. Vo, and K. Dietmayer, "The labeled multi-Bernoulli filter," *IEEE Trans. Signal Process.*, vol. 62, no. 12, pp. 3246–3260, Dec. 2014.
[12] C. Fantacci and F. Papi, "Scalable multisensor multitarget tracking using the marginalized δ-GLMB density," *IEEE Signal Process. Lett.*, vol. 23, no. 6, pp. 863–867, Jun. 2016.
[13] H. G. Hoang, B.-T. Vo, and B.-N. Vo, "A fast implementation of the generalized labeled multi-Bernoulli filter with joint prediction and update," in *Proc. 18th Int. Conf. Inf. Fusion*, Washington, DC, USA, Jul. 2015, pp. 999–1006.
[14] B.-N. Vo, B.-T. Vo, and H. G. Hoang, "An efficient implementation of the generalized labeled multi-Bernoulli filter," *IEEE Trans. Signal Process.*, vol. 65, no. 8, pp. 1975–1987, Apr. 2017.
[15] Z. B. Liang, F. X. Liu, L. Y. Li, and J. L. Gao, "Improved generalized labeled multi-Bernoulli filter for non-ellipsoidal extended targets or group targets tracking based on random sub-matrices," *Digit. Signal Process.*, vol. 99, pp. 1–25, Apr. 2020.
[16] B.-N. Vo and B.-T. Vo, "An implementation of the multi-sensor generalized labeled multi-Bernoulli filter via Gibbs sampling," in *Proc. 20th Int. Conf. Inf. Fusion (Fusion)*, Xi'an, China, Jul. 2017, pp. 1–8.
[17] B.-N. Vo, B.-T. Vo, and M. Beard, "Multi-sensor multi-object tracking with the generalized labeled multi-Bernoulli filter," *IEEE Trans. Signal Process.*, vol. 67, no. 23, pp. 5952–5967, Dec. 2019.
[18] M. Beard, B. T. Vo, and B.-N. Vo, "A solution for large-scale multi-object tracking," *IEEE Trans. Signal Process.*, vol. 68, pp. 2754–2769, 2020.
[19] Y. G. Punchihewa, B.-T. Vo, B.-N. Vo, and D. Y. Kim, "Multiple object tracking in unknown backgrounds with labeled random finite sets," *IEEE Trans. Signal Process.*, vol. 66, no. 11, pp. 3040–3055, Jun. 2018.
[20] B.-N. Vo and B.-T. Vo, "A multi-scan labeled random finite set model for multi-object state estimation," *IEEE Trans. Signal Process.*, vol. 67, no. 19, pp. 4948–4963, Oct. 2019.
[21] I. Bilik and J. Tabrikian, "Maneuvering target tracking in the presence of glint using the nonlinear Gaussian mixture Kalman filter," *IEEE Trans. Aerosp. Electron. Syst.*, vol. 46, no. 1, pp. 246–262, Jan. 2010.
[22] G. A. Hewer, R. D. Martin, and J. Zeh, "Maneuvering target tracking in the presence of glint using the nonlinear Gaussian mixture Kalman filter," *IEEE Trans. Aerosp. Electron. Syst.*, vol. AES-23, no. 1, pp. 120–128, Jan. 1987.
[23] W.-R. Wu and D.-C. Chang, "Feedback median filter for robust preprocessing of glint noise," *IEEE Trans. Aerosp. Electron. Syst.*, vol. 36, no. 4, pp. 1026–1035, Oct. 2000.
[24] W.-R. Wu, "Target racking with glint noise," *IEEE Trans. Aerosp. Electron. Syst.*, vol. 29, no. 1, pp. 174–185, Jan. 1993.
[25] J. Kim, M. Tandale, P. K. Menon, and E. Ohlmeyer, "Particle filter for ballistic target tracking with glint noise," *J. Guid., Control, Dyn.*, vol. 33, no. 6, pp. 1918–1921, Nov. 2010.
[26] M. Wüthrich, C. G. Cifuentes, S. Trimpe, F. Meier, J. Bohg, J. Issac, and S. Schaal, "Robust Gaussian filtering using a pseudo measurement," in *Proc. Amer. Control Conf. (ACC)*, Boston, MA, USA, Jul. 2016, pp. 3606–3613.

[27] J. Christmas and R. Everson, "Robust autoregression: Student-t innovations using variational Bayes," *IEEE Trans. Signal Process.*, vol. 59, no. 1, pp. 48–57, Jan. 2011.
[28] E. Daeipour and Y. Bar-Shalom, "An interacting multiple model approach for target tracking with glint noise," *IEEE Trans. Aerosp. Electron. Syst.*, vol. 31, no. 2, pp. 706–715, Apr. 1995.
[29] L. Hou, F. Lian, G. T. F. D. Abreu, and S. Tan, "Robust δ-generalized labeled multi-Bernoulli filter for nonlinear systems with heavy-tailed noises," in *Proc. 23th Int. Inf. Fusion*, Rustenburg, South Africa, Jul. 2020, pp. 1–8.
[30] W. Li, Y. Jia, J. Du, and J. Zhang, "PHD filter for multi-target tracking with glint noise," *Signal Process.*, vol. 94, pp. 48–56, Jan. 2014.
[31] C. Li, R. Wang, Y. Hu, and J. Wang, "Cardinalised probability hypothesis density tracking algorithm for extended objects with glint noise," *IET Sci., Meas. Technol.*, vol. 10, no. 5, pp. 528–536, Aug. 2016.
[32] P. Dong, Z. Jing, H. Leung, K. Shen, and M. Li, "The labeled multi-Bernoulli filter for multitarget tracking with glint noise," *IEEE Trans. Aerosp. Electron. Syst.*, vol. 55, no. 5, pp. 2253–2268, Oct. 2019.
[33] P. Dong, Z. Jing, H. Leung, K. Shen, and J. Wang, "Student-t mixture labeled multi-Bernoulli filter for multi-target tracking with heavy-tailed noise," *Signal Process.*, vol. 152, pp. 331–339, Nov. 2018.
[34] Z.-X. Liu and B.-J. Huang, "The labeled multi-Bernoulli filter for jump Markov systems under glint noise," *IEEE Access*, vol. 7, pp. 92322–92328, 2019.
[35] Y. Huang, G. Jia, B. Chen, and Y. Zhang, "A new robust Kalman filter with adaptive estimate of time-varying measurement bias," *IEEE Signal Process. Lett.*, vol. 27, pp. 700–704, 2020.
[36] B. Borden and M. Mumford, "A statistical glint/radar cross section target model," *IEEE Trans. Aerosp. Electron. Syst.*, vol. AES-19, no. 5, pp. 781–785, Sep. 1983.
[37] S. Kotz and S. Nadarajah, *Multivariate T Distributions and Their Applications*. Cambridge, U.K.: Cambridge Univ. Press, 2004, ch. 2, pp. 36–38.
[38] M.-A. Sato, "Online model selection based on the variational Bayes," *Neural Comput.*, vol. 13, no. 7, pp. 1649–1681, Jul. 2001.
[39] C. M. Bishop, *Pattern Recognition and Machine Learning*. New York, NY, USA: Springer, 2007, ch. 10, pp. 518–521.
[40] D. Schuhmacher, B.-T. Vo, and B.-N. Vo, "A consistent metric for performance evaluation of multi-object filters," *IEEE Trans. Signal Process.*, vol. 56, no. 8, pp. 3447–3457, Aug. 2008.
[41] M. Beard, B. T. Vo, and B.-N. Vo, "Performance evaluation for large-scale multi-target tracking algorithms," in *Proc. 21st Int. Conf. Inf. Fusion (FUSION)*, Cambridge, U.K., Jul. 2018, pp. 1–5.

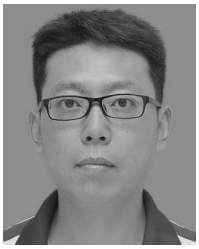

LIMING HOU received the M.S. degree in pattern recognition and intelligent system from the Sichuan University of Science and Engineering, Zigong, China, in 2014. He is currently pursuing the Ph.D. degree with the School of Electronics and Information Engineering, Xi'an Jiaotong University, Xi'an, China. His research interests include target tracking, information fusion, and sensor management.

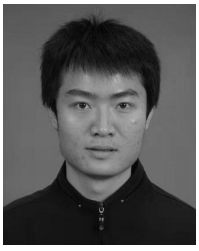

FENG LIAN received the B.S. and Ph.D. degrees from the School of Electronics and Information Engineering, Xi'an Jiaotong University, Xi'an, China, in 2004 and 2009, respectively. He is currently a Professor with the School of Electronics and Information Engineering, Xi'an Jiaotong University. His research interests include target tracking, information fusion, and sensor management.

SHUNCHENG TAN received the B.S. degree in electronic engineering and the Ph.D. degree in information and communication engineering from Naval Aeronautical and Astronautical University, Yantai, China, in 2008 and 2014, respectively. He is currently a Lecturer with the Institute of Information Fusion Technology, Naval Aeronautical and Astronautical University. His research interests include information fusion and radar information processing.

CONGAN XU received the B.S. degree in electronic engineering and the Ph.D. degree in information and communication engineering from Naval Aeronautical and Astronautical University, Yantai, China, in 2010 and 2017, respectively. He is currently a Lecturer with the Institute of Information Fusion Technology, Naval Aeronautical and Astronautical University. His research interests include multisensor information fusion and intelligent information processing.

GIUSEPPE THADEU FREITAS DE ABREU (Senior Member, IEEE) received the B.Eng. degree in electrical engineering and the Specialization degree in telecommunications engineering from the Universidade Federal da Bahia, Salvador, Brazil, in 1996 and 1997, respectively, and the M.Eng. and D.Eng. degrees in physics, electrical and computer engineering from Yokohama National University, Japan, in March 2001 and March 2004, respectively. He was a Postdoctoral Fellow and later an Adjunct Professor on statistical signal processing and communications theory at the Department of Electrical and Information Engineering, University of Oulu, Finland, from 2004 to 2006 and from 2006 to 2011, respectively. Since 2011, he has been a Professor of electrical engineering with Jacobs University Bremen, Germany. His research interests include communications theory, estimation theory, statistical modeling, wireless localization, cognitive radio, wireless security, compressive sensing, and energy harvesting networks.